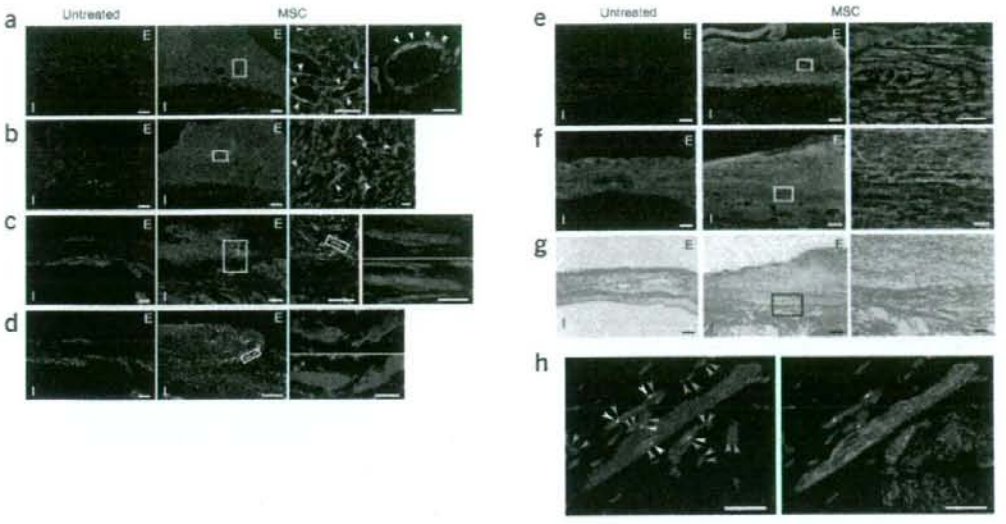

Figure 4 Differentiation of MSCs within the MSC tissue after growth *in situ*. (**a**,**b**) GFP-expressing MSCs (green) were identified as a thick stratum at the epicardial side of the myocardium. The MSC tissue contained a number of vascular structures positive for vWF (red, **a**) and αSMA (red, **b**). MSCs that did not participate in blood vessel formation were only rarely positive for αSMA, a marker for myofibroblasts. Arrows indicate transplanted MSCs positive for vWF or αSMA. (**c**,**d**) Some MSCs within the MSC tissue were positive for cardiac markers cardiac troponin T (red, **c**) and desmin (red, **d**). (**e**) Most of the MSC tissue was positive for vimentin (red). (**f**) The MSC tissue modestly stained for collagen type 1 (red). (**g**) Collagen deposition was also detected by picrosirius red staining. (**h**) FISH analysis. Newly formed cardiomyocytes (desmin, red) that were positive for GFP (green) had only one set of X (purple) and Y chromosomes (white), whereas two X chromosomes were detected exclusively in GFP^- host-derived cells. Nuclei are stained with DAPI (blue, **a**–**f** and **h**). Scale bars in left three panels of **a** and **c** and in two left panels of **b** and **d**–**g**, 100 μm; in **h** and far right panels of **a**–**g**, 20 μm. E, epicardial side; I, intimal side.

In summary, adipose tissue–derived monolayered MSCs can be readily engrafted to the scarred myocardium, grow gradually *in situ* and become a thick stratum that includes newly formed vessels, cardiomyocytes and undifferentiated MSCs. The engrafted MSCs reversed wall thinning in the scar area and improved cardiac function and survival in rats with myocardial infarction. Thus, transplantation of monolayered MSCs may be a new therapeutic strategy for cardiac tissue regeneration.

METHODS

Model of heart failure. All protocols were performed in accordance with the guidelines of the Animal Care Ethics Committee of the Japanese National Cardiovascular Center Research Institute. We used male Sprague-Dawley rats (Japan SLC) weighing 187–215 g. A myocardial infarction model was produced by ligation of the left coronary artery, as described previously[30]. Briefly, we anesthetized rats with sodium pentobarbital (30 mg/kg) and ventilated them with a volume-regulated respirator. We exposed hearts by left thoracotomy, and ligated the left coronary artery 2–3 mm from its origin between the pulmonary artery conus and the left atrium with a 6-0 Prolene suture. The sham group underwent thoracotomy and cardiac exposure without coronary ligation. The surviving rats were maintained on standard rat chow.

Study protocol. We randomly placed rats into four groups: rats with chronic heart failure that underwent transplantation of monolayered MSCs (MSC group; $n = 12$), rats with chronic heart failure given monolayered DFBs (DFB group; $n = 12$), rats with chronic heart failure without transplantation (untreated group; $n = 12$) and sham-operated rats without transplantation (sham group; $n = 10$). Four weeks after coronary ligation, the MSC and DFB groups underwent autologous transplantation of each monolayered cell graft onto the anterior wall, including the scar area (**Supplementary Methods** online). The other two groups underwent the same operative procedures without transplantation. We performed hemodynamic studies, echocardiography and histological assessments 4 and 8 weeks after coronary ligation (**Supplementary Methods**). Upon killing at 8 weeks after coronary ligation, only those rats with infarct size > 25% of the left ventricle area were included in this study. Therefore, the variation in infarct size between the experimental rats was relatively low (28–41%, average 33.9% ± 1.9%).

Isolation and culture of MSCs from adipose tissue. Immediately after coronary ligation, we acquired subcutaneous adipose tissue (1.1 ± 0.1 g) from the right inguinal region of each rat. We minced adipose tissue with scissors and digested it with 10 ml of type 1 collagenase solution (0.1 mg/ml, Worthington Biochemical) for 1 h in a 37 °C water bath shaker. After filtration with mesh filter (Costar 3480, Corning) and centrifugation at 780*g* for 8 min, we suspended isolated cells in α-MEM supplemented with 10% FCS and antibiotics, plated them onto a 100-mm dish and incubated them at 37 °C with 5% CO_2. A small number of spindle-shaped cells were apparent in visible symmetric colonies by days 5–7.

Preparation of temperature-responsive dishes. Specific procedures for preparation of square-designed PIPAAm-grafted dishes have been previously described[9]. Briefly, we spread IPAAm monomer (Kohjin) in 2-propanol solution onto 60-mm polystyrene culture dishes (Corning). We then subjected the dishes to irradiation (0.25-MGy electron beam dose) using an Area Beam Electron Processing system (Nisshin High-Voltage) to immobilize IPAAm on the dish surface; we then rinsed dishes with cold distilled water and dried them in nitrogen gas. In the second step, we masked the PIPAAm-grafted surface with a square glass coverslip (24 × 24 mm, Matsunami Glass). We spread acrylamide (AAm) monomer solution in 2-propanol onto the masked dish surface. We then irradiated the dish surface with an electron beam and washed it. As a result, the central square area of each dish was PIPAAm grafted (temperature responsive), and the surrounding border was poly-AAm grafted (non–cell adhesive). This PIPAAm-grafted surface is hydrophobic under culture

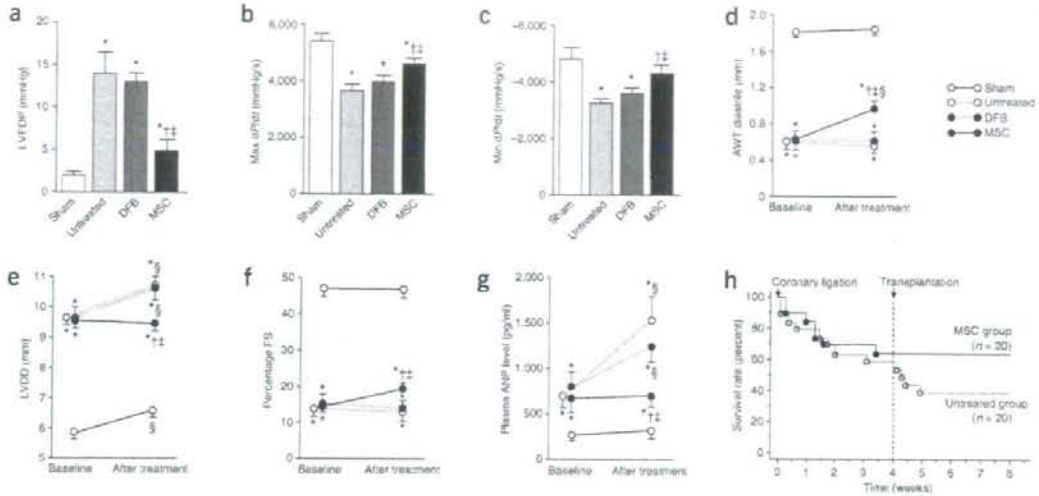

Figure 5 Cardiac structure and function after transplantation of monolayered MSCs. (**a–c**) Hemodynamic parameters obtained by catheterization. LVEDP, left ventricle end-diastolic pressure. (**d–f**) Echocardiographic findings. AWT, anterior wall thickness; LVDD, left ventricle end-diastolic dimension; FS, fractional shortening. (**g**) Plasma atrial natriuretic peptide (ANP) level. Baseline represents measurements 4 weeks after coronary ligation; 'after treatment' represents measurements taken 4 weeks after transplantation (8 weeks after coronary ligation). Data are mean ± s.e.m. $^{*}P < 0.05$ versus sham group; $^{\dagger}P < 0.05$ versus untreated group; $^{\ddagger}P < 0.05$ versus DFB group; $^{\S}P < 0.05$ versus baseline. (**h**) Survival of rats with chronic heart failure with or without monolayered MSC transplantation. The Kaplan-Meier survival curve demonstrates an 8-week survival rate of 65% for the MSC group versus 45% for the untreated group. Survival rate after transplantation was significantly higher in the MSC group than in the untreated group (100% versus 71% 4-week survival rate after transplantation, log-rank test, $P < 0.05$).

conditions at 37 °C and becomes reversibly hydrophilic below 32 °C. Therefore, cultured cells that adhere to the dish surface spontaneously detach from the grafted surface without enzymatic digestion.

Preparation of monolayered cell grafts. We suspended MSCs at the third or fourth passage from adipose tissue or DFBs at the second passage by trypsinization, and plated the cell suspension containing 3 ml of complete medium onto a 60-mm temperature-responsive dish at 5×10^5 cells per dish (MSCs) or 8×10^5 cells per dish (DFBs) and cultured cells at 37 °C. After 3 d of culture, confluently cultured MSCs or DFBs on the temperature-responsive dishes were incubated at 20 °C. By 40 min, both MSCs and DFBs detached spontaneously and floated up into the medium as monolayered cell grafts. Immediately after detachment, we gently aspirated the monolayered cell grafts using a 1,000 μl pipette tip and transferred them onto an elastic plastic sheet.

Statistical analysis. Numerical values are expressed as mean ± s.e.m. There are four groups of continuous variables in this study. Therefore, for multiple comparisons of more than two groups, we performed one-way analysis of variance (ANOVA). If the ANOVA was significant, we used the Newman-Keul procedure as a *post hoc* test. For repeated measurement such as echocardiographic parameters, we performed two-way repeated ANOVA with the Newman-Keul test. Comparisons of parameters between two groups were made by unpaired Student *t*-test. A value of $P < 0.05$ was considered significant.

Note: Supplementary information is available on the Nature Medicine website.

ACKNOWLEDGMENTS

We thank J.I. Hoffman for his statistical advice. We thank T. Iwase, T. Ito, S. Murakami, N. Sakata and Y. Isono for their technical support. We thank Y. Tsuboi and H. Sonoda for their assistance with microscopic analysis of monolayered cell grafts. We also thank Y. Sawa for his suggestions on this study. This work was supported by research grants for Cardiovascular Disease (16C-6) and Human Genome Tissue Engineering 005 and 009 from the Japanese Ministry of Health, Labor and Welfare, and the Program for Promotion of Fundamental Studies in Health Science of the Japanese National Institute of Biomedical Innovation.

COMPETING INTERESTS STATEMENT

The authors declare competing financial interests (see the *Nature Medicine* website for details).

Published online at http://www.nature.com/naturemedicine/
Reprints and permissions information is available online at http://npg.nature.com/reprintsandpermissions/

1. Liu, J. *et al.* Autologous stem cell transplantation for myocardial repair. *Am. J. Physiol. Heart Circ. Physiol.* **287**, H501–H511 (2004).
2. Reinlib, L. & Field, L. Cell transplantation as future therapy for cardiovascular disease?: A workshop of the National Heart, Lung, and Blood Institute. *Circulation* **101**, E182–E187 (2000).
3. Schuster, M.D. *et al.* Myocardial neovascularization by bone marrow angioblasts results in cardiomyocyte regeneration. *Am. J. Physiol. Heart Circ. Physiol.* **287**, H525–H532 (2004).
4. Kocher, A.A. *et al.* Neovascularization of ischemic myocardium by human bone-marrow-derived angioblasts prevents cardiomyocyte apoptosis, reduces remodeling and improves cardiac function. *Nat. Med.* **7**, 430–436 (2001).
5. Bel, A. *et al.* Transplantation of autologous fresh bone marrow into infarcted myocardium: a word of caution. *Circulation* **108**, II247–II252 (2003).
6. Yamada, N. *et al.* Thermo-responsive polymeric surface: control of attachment and detachment of cultured cells. *Makromol. Chem. Rapid Commun.* **11**, 571–576 (1990).
7. Okano, T., Yamada, H., Sakai, H. & Sakurai, Y. A novel recovery system for cultured cells using plasma-treated polystyrene dishes grafted with poly (N-isopropylacrylamide). *J. Biomed. Mater. Res.* **27**, 1243–1251 (1993).
8. Shimizu, T. *et al.* Fabrication of pulsatile cardiac tissue grafts using a novel 3-dimensional cell sheet manipulation technique and temperature-responsive cell culture surfaces. *Circ. Res.* **90**, e40–e48 (2002).
9. Hirose, M., Kwon, O.H., Yamato, M., Kikuchi, A. & Okano, T. Creation of designed shape cell sheets that are noninvasively harvested and moved onto another surface. *Biomacromolecules* **1**, 377–381 (2000).
10. Kushida, A. *et al.* Decrease in culture temperature releases monolayer endothelial cell sheets together with deposited fibronectin matrix from temperature-responsive culture surfaces. *J. Biomed. Mater. Res.* **45**, 355–362 (1999).
11. Herreros, J. *et al.* Autologous intramyocardial injection of cultured skeletal muscle-derived stem cells in patients with non-acute myocardial infarction. *Eur. Heart J.* **24**, 2012–2020 (2003).

12. Skobel, E. *et al.* Transplantation of fetal cardiomyocytes into infarcted rat hearts results in long-term functional improvement. *Tissue Eng.* **10**, 849–864 (2004).
13. Hodgson, D.M. *et al.* Stable benefit of embryonic stem cell therapy in myocardial infarction. *Am. J. Physiol. Heart Circ. Physiol.* **287**, H471–H479 (2004).
14. Makino, S. *et al.* Cardiomyocytes can be generated from marrow stromal cells in vitro. *J. Clin. Invest.* **103**, 697–705 (1999).
15. Pittenger, M.F. *et al.* Multilineage potential of adult human mesenchymal stem cells. *Science* **284**, 143–147 (1999).
16. Reyes, M. *et al.* Origin of endothelial progenitors in human postnatal bone marrow. *J. Clin. Invest.* **109**, 337–346 (2002).
17. Toma, C., Pittenger, M.F., Cahill, K.S., Byrne, B.J. & Kessler, P.D. Human mesenchymal stem cells differentiate to a cardiomyocyte phenotype in the adult murine heart. *Circulation* **105**, 93–98 (2002).
18. Wang, J.S. *et al.* Marrow stromal cells for cellular cardiomyoplasty: feasibility and potential clinical advantages. *J. Thorac. Cardiovasc. Surg.* **120**, 999–1005 (2000).
19. Jiang, Y. *et al.* Pluripotency of mesenchymal stem cells derived from adult marrow. *Nature* **418**, 41–49 (2002).
20. Nagaya, N. *et al.* Transplantation of mesenchymal stem cells improves cardiac function in a rat model of dilated cardiomyopathy. *Circulation* **112**, 1128–1135 (2005).
21. Rangappa, S., Fen, C., Lee, E.H., Bongso, A. & Wei, E.S. Transformation of adult mesenchymal stem cells isolated from the fatty tissue into cardiomyocytes. *Ann. Thorac. Surg.* **75**, 775–779 (2003).
22. Zuk, P.A. *et al.* Human adipose tissue is a source of multipotent stem cells. *Mol. Biol. Cell* **13**, 4279–4295 (2002).
23. Gaustad, K.G., Boquest, A.C., Anderson, B.E., Gerdes, A.M. & Collas, P. Differentiation of human adipose tissue stem cells using extracts of rat cardiomyocytes. *Biochem. Biophys. Res. Commun.* **314**, 420–427 (2004).
24. Planat-Benard, V. *et al.* Plasticity of human adipose lineage cells toward endothelial cells: physiological and therapeutic perspectives. *Circulation* **109**, 656–663 (2004).
25. Lee, R.H. *et al.* Characterization and expression analysis of mesenchymal stem cells from human bone marrow and adipose tissue. *Cell. Physiol. Biochem.* **14**, 311–324 (2004).
26. Li, J., Takaishi, K., Cook, W., McCorkle, S.K. & Unger, R.H. Insig-1 "brakes" lipogenesis in adipocytes and inhibits differentiation of preadipocytes. *Proc. Natl. Acad. Sci. USA* **100**, 9476–9481 (2003).
27. Vande Berg, J.S., Rudolph, R. & Woodward, M. Comparative growth dynamics and morphology between cultured myofibroblasts from granulating wounds and dermal fibroblasts. *Am. J. Pathol.* **114**, 187–200 (1984).
28. Nishida, K. *et al.* Corneal reconstruction with tissue-engineered cell sheets composed of autologous oral mucosal epithelium. *N. Engl. J. Med.* **351**, 1187–1196 (2004).
29. Shimizu, T., Yamato, M., Kikuchi, A. & Okano, T. Cell sheet engineering for myocardial tissue reconstruction. *Biomaterials* **24**, 2309–2316 (2003).
30. Nishikimi, T., Uchino, K. & Frohlich, E.D. Effects of α1-adrenergic blockade on intrarenal hemodynamics in heart failure rats. *Am. J. Physiol. Regul. Integr. Comp. Physiol.* **262**, R198–R203 (1998).

Journal of Cellular Physiology

Highly Efficient and Feeder-Free Production of Subculturable Vascular Endothelial Cells From Primate Embryonic Stem Cells

KUMIKO SAEKI,[1] YOSHIKO YOGIASHI,[1] MASAKO NAKAHARA,[1] NAOKO NAKAMURA,[1] SATOKO MATSUYAMA,[1] AKEMI KOYANAGI,[2] HIDEO YAGITA,[2] MAKOTO KOYANAGI,[1] YASUSHI KONDO,[3] AND AKIRA YUO[1]*

[1]*Department of Hematology, Research Institute, International Medical Center of Japan, Tokyo, Japan*

[2]*Department of Immunology, Juntendo University School of Medicine, Tokyo, Japan*

[3]*Regenerative Medicine Group, Advanced Medical Research Laboratory, Mitsubishi Tanabe Pharma Corporation, Osaka, Japan*

The vascular endothelial cell (VEC) differentiation from primate embryonic stem (ES) cells has critical problems: low differentiation efficiencies (<2%) and/or subculture incapability. We report a novel feeder-free culture method for high efficiency production of subculturable VECs from cynomolgus monkey ES cells. Spheres, which were generated from ES cells in the presence of cytokine cocktail, were cultured on gelatin-coated plates. Cobblestone-shaped cells spread out after a few days, which were followed by an emergence of a sac-like structure containing hematopoietic cells. All adherent cells including sac walls cells and surrounding cobblestone cells expressed vascular endothelial cadherin (VE-cadherin) at intercellular junctions. Subculture of these cells resulted in a generation of homogeneous spindle-shaped population bearing cord-forming activities and a uniform acetylated low density lipoprotein-uptaking capacity with von Willbrand factor and endothelial nitric oxide synthetase expressions. They were freeze–thaw-tolerable and subculturable up to eight passages. Co-existence of pericytes or immature ES cells was ruled out. When introduced in a collagen sponge plug implanted intraperitoneally in mice, ES-derived cells recruited into neovascularity. Although percentages of surface VE-cadherin-positive population varied from 20% to 80% as assessed by flow cytometry, the surface VE-cadherin-negative population showed intracellular VE-cadherin expression and mature functions, as we call it as atypical VECs. When sorted, the surface VE-cadherin-positive population expanded as almost pure (>90%) VE-cadherin/PECAM-1-positive VECs by 160-fold after five passages. Thus, our system provides pure production of functional, subculturable and freeze–thaw-tolerable VECs, including atypical VECs, from primate ES cells.

J. Cell. Physiol. 217: 261–280, 2008.

Embryonic stem (ES) cells are a valuable resource in regenerative medicine because of their high capacity to differentiate into a broad range of cell types. It has been revealed that primate ES cells have characteristics distinct from those of murine ES cells. For example, leukemia inhibitory factor is ineffective for maintaining the immaturity of human ES cells (Sato et al., 2004). The gene expression patterns also differ between primate and murine ES cells. For example, undifferentiated primate ES cells express kinase insert domain receptor (KDR, Flk-1, a type 2 receptor for vascular endothelial growth factor (VEGF-R2)) although undifferentiated murine ES cells do not (Sone et al., 2003; Vodyanik et al., 2005). KDR is known as an excellent marker for sorting the vascular endothelial precursor population in murine ES differentiation system (Yamashita et al., 2000). However, the presence of KDR in undifferentiated primate ES cells limits a direct application of the murine system to the primate one (Sone et al., 2003). Eventually, by contrast to the highly efficient production (>90%) of vascular endothelial cells from murine ES cells (Hirashima et al., 1999), that from primate ES cells is significantly low; the efficiency of the production of vascular endothelial cadherin (VE-cadherin)-positive (Sone et al., 2003, 2007) or platelet endothelial cell adhesion molecule-1 (PECAM-1)-positive (Levenberg et al., 2002) cell are not higher than two percents. Although the human ES cell study is essential for clinical application, basic researches using monkey ES cells still has great importance because they provide good transplantation models that must be performed in the pre-clinical study (Takagi et al., 2005). Moreover, the use of monkey ES cells avoids ethical issues and thus the biotechnological manipulation of them, including gene transfer, can immediately be applied, which will contribute to understand human ES cells.

Currently, there are three major methods for the in vitro differentiation of ES cells into specific lineages. One is co-culturing ES cells with stromal cells as their feeders (Hirashima et al., 1999; Sone et al., 2003, 2007). Feeder cells have large capacities to promote directed differentiation and to support viability of differentiated cells. Nevertheless, contamination of the final product by feeder cells is inevitable, and thus, an especially strict cell-sorting technique is required for purification of the final products. Concerning vascular endothelial differentiation of primate ES cells, however, the efficiency of cell surface VE-cadherin-positive cell production is considerably low (<2%) even when murine OP9 feeder cells were used (Sone et al., 2003, 2007). Besides, massive

Contract grant sponsor: The Japan Health Sciences Foundation; Contract grant number: KH61061.

*Correspondence to: Akira Yuo, Department of Hematology, Research Institute, International Medical Center of Japan, 1-21-1, Toyama, Shinjuku-ku, Tokyo 162-8655, Japan.
E-mail: yuoakira@ri.imcj.go.jp

Received 22 December 2007; Accepted 23 April 2008

DOI: 10.1002/jcp.21502

contamination of pericytes reportedly occurs in this system. Pericytes are important players for angiogenesis, and thus, the co-generation of pericytes might be beneficial in some aspects. However, domination of pericytes after passages considerably hinder the pure expansion of vascular endothelial cells even after sorting of VE-cadherin-positive cells (Sone et al., 2007). The second method is a feeder-free culture via a generation of embryoid bodies (EBs) or spheres (Levenberg et al., 2002). It is beneficial that it can exclude the risk of contamination of xenogenic materials. Yet, directions of differentiation in EBs or spheres are principally random and cannot easily be focused on a specific lineage. As a result, fairly large volumes of starting ES cells are required to obtain sufficient amounts of differentiated cells. Additionally, these two methods described above share a common disadvantage; they do not provide a clear microscopic field for observation and manipulation due to co-existing feeder cells or the compact three-dimensional structures of EBs or spheres. The third method is a simple adherent culture of ES cells. There have been two reports concerning this method. One is the continual culture of rhesus monkey ES (rmES) cells on mouse embryonic fibroblasts (MEFs) using a vascular endothelial cell-specific culture medium of EGM®-2 MV BulletKit (Kaufman et al., 2004). This system provided a good microscopic field and effectively produced the subculturable vascular endothelial cells. However, these cells are not the conventional or canonical vascular endothelial cells, but rather, seem to be "atypical" vascular endothelial cells in that neither the expression of VE-cadherin, a vascular endothelial cell-specific and pan-vascular endothelial marker, nor PECAM-1, a mature vascular endothelial cell marker, was detected by flow cytometry. Nonetheless, they have mature endothelial functions including in vitro cord-forming and acetylated low density lipoprotein (Ac-LDL)-uptaking activities and in vivo neovascularization activity along with expressions of von Willbrand factor (vWF) and endothelial nitric oxide synthetase (eNOS). The other one is an adherent culture of human ES-derived CD34-positive cells, which were spontaneously generated by overgrown ES cells on MEFs in the presence of serum, in EGM®-2 MV BulletKit (Wang et al., 2007). This system requires the enrichment of CD34-positive cells (<10%) by cell sorter before subsequent culture in EGM®-2 MV BulletKit. Although this system provides VE-cadherin-positive functional vascular endothelial cells, they are not subculturable. Thus, the most urgent task for the vascular endothelial differentiation from primate ES cells is to establish a method for "feeder-free" and "high efficiency" production for cell surface "VE-cadherin-positive" and "subculturable" vascular endothelial cells.

Here we report a novel method for highly efficient production of functional, subculturable, freeze–thaw-tolerable and cell-surface-VE-cadherin-positive vascular endothelial cells from cynomolgus monkey ES (cmES) cells in feeder-free culture system. Furthermore, it does not require a step to enrich the progenitor fractions, such as CD34-positive and/or KDR-positive fractions, by cell sorter. To our knowledge, this is the highest efficiency system for the production of vascular endothelial cells. Indeed, our system provides almost two pure populations: the cell surface VE-cadherin-positive canonical vascular endothelial cells and cell surface VE-cadherin-negative "atypical" vascular endothelial cells. The characterization and significance of these atypical vascular endothelial cells is referred and discussed in this report.

Materials and Methods

Cells and reagents

Murine embryonic fibroblasts (MEFs), which had been treated with Dulbecco's modified Eagle's medium (DMEM) containing mitomycin C (MMC) (Sigma Chemical Co., St. Louis, MO) for 3 h, were seeded on the dishes coated with 0.1% gelatin. The cmES cells (CMK-6) (Suemori et al., 2001) were maintained on MMC-treated MEF-coated dishes in DMEM/F12 medium (Invitrogen Corp., Carslbad, CA) supplemented with 20% Knockout™ Serum Replacement (KSR™, Invitrogen Corp.), 1% Non-essential amino acids solution (Invitrogen Corp.), 1 mM Sodium Pyruvate Solution (Invitrogen Corp.), 2 mM L-glutamine (Invitrogen Corp.), 10 U/ml penicillin (Invitrogen Corp.) and 10 μg/ml streptomycin (Invitrogen Corp.). ES cells were passed twice a week by collagenase treatment and seeded at split ratios of 1:2 to 1:4 on new MEF-coated dishes. Human aortic endothelial cells (HAEC) and human umbilical vein endothelial cells (HUVEC) were purchased from Lonza Group Ltd. (Basel, Switzerland), and maintained on gelatin-coated dishes using EGM®-2 BulletKit (Lonza Group Ltd.). Normal Human Aortic Smooth Muscle cells (AOSMC)) were purchased from Lonza Group Ltd. and maintained on gelatin-coated dishes using SmGM®-2 BulletKit® (Lonza Group Ltd.). The human leukemic UT-7 and HL-60 cells were cultured RPMI 1640 medium (Sigma Chemical Co.) supplemented with 10% heat-inactivated fetal bovine serum (FBS).

Differentiation procedure

ES colonies were collected by collagenase treatment without a contamination of MEFs and further disaggregated by trypsinization. Cell aggregates were generated by a hanging drop culture, where 3,000 cmES cells were incubated in a 30 μl drop of differentiation medium (DM) consisting of Iscove's modified Dulbecco's medium (IMDM) (Sigma Chemical Co.) supplemented with 15% heat-inactivated FBS (PAA Laboratories GmbH, Linz, Austria), 0.1 mM β-mercaptoethanol (Sigma Chemical Co.), 3 mM L-glutamine (Invitrogen Corp.), 10 U/ml penicillin (Invitrogen Corp.), 20 ng/ml vascular endothelial growth factor (VEGF; Pepro Tech Inc., Rocky Hill, NJ), 20 ng/ml bone morphogenic protein 4 (BMP-4; R&D Systems Inc., Minneapolis, MN), 20 ng/ml stem cell factor (SCF; Pepro Tech Inc.), 10 ng/ml Flt3 ligand (Flt3-L; Pepro Tech Inc.), 20 ng/ml interleukin 3 (IL-3; Pepro Tech Inc.) and 10 ng/ml interleukin 6 (IL-6; Pepro Tech Inc.). After incubating the drops for 3 days at 37°C under a 100% humidified condition in a 5% CO_2 gas incubator, cell aggregates generated from 72 hanging drops were subjected to adherent culture on a 100 mm × 20 mm gelatin-coated dishes using differentiation medium described. Media were changed twice a week. After about 2 weeks, a VE-cadherin-positive sac-like structure filled with round cells along with surrounding VE-cadherin-positive cobblestone cells emerged. Before sacs were fully packed by inner round cells, sac walls were manually cut by using stem cell knife (Vitrolife AB, Kungsbacka, Sweden) under microscopic observation. After releasing the inner round cells into culture supernatant, total adherent cells including fragmented sac walls and surrounding cobblestone cells were massively transferred onto new gelatin-coated dishes via trypsin/EDTA treatment. These cells were subcultured by 1:3 dilution twice a week. In some experiments, EGM®-2 BulletKit (Lonza Group Ltd.) was used in place of the differentiation medium described above throughout the differential processes including hanging drop culture and subsequent adherent culture.

Morphological and cytochemical examinations

Viable cells were directly observed under an inverted phase contrast light microscope (Olympus Optical Co. Ltd., Tokyo, Japan), or alternatively, cells were fixed on slide glasses using a cytospin apparatus (Cytospin 2, SHANDON, Pittsburgh, PA), stained with Wright-Giemsa solution, myeloperoxidase staining kit or esterase staining kit (Muto Pure Chemical Co., Tokyo, Japan), and then observed under the light microscope (Olympus Optical Co. Ltd.).

Flow cytometric analyses and cell sorting

Cells were collected by 0.2% EDTA treatment and, after a wash in phosphate-buffered saline (PBS), 1×10^6 cells were reacted with first antibodies on ice for 30 min. The expression level of each protein was analyzed using a FACSCalibur™ (BD Biosciences, San Jose, CA). The antibodies used were a mouse monoclonal anti-human VE-cadherin (clone TEA1/31)-phycoerythrin (PE) antibody (Beckman Coulter Inc., Fullerton, CA), a mouse monoclonal anti-human CD31 (PECAM-1)-fluorescein isothiocyanate (FITC) antibody (clone WM59) (BD Biosciences), a mouse monoclonal anti-human CD34 (clone 563)-PE antibody (BD Biosciences), a mouse monoclonal anti-human Tie-2 (clone 83715)-PE (R&D Systems Inc.), a mouse monoclonal anti-human VEGF-R1 (Flt-1) (clone 49560)-PE antibody (R&D Systems Inc.), a mouse monoclonal anti-human VEGF-R2 (KDR, Flk-1) (clone 89106)-PE antibody (R&D Systems Inc.), a mouse monoclonal anti-human VEGF-R3 (Flt-4) (clone 54733)-PE antibody (R&D Systems Inc.), a mouse monoclonal anti-human CD14 (clone M5E2)-PE antibody (BioLegend, San Diego, CA), a mouse monoclonal anti-human CD18 (clone 6.7)-FITC antibody (BD Biosciences), a mouse monoclonal anti-human CD11b (clone ICRF44)-PE antibody (BD Biosciences) and a mouse monoclonal anti-human CD45 (clone TÜ116)-PE antibody (BD Biosciences). As for the anti-VE-cadherin antibody reaction, secondary antibody reaction was performed using a goat anti-mouse IgG-PE (Calbiochem Co., La Jolla, CA). After antibody-staining procedures, cells were stained with TO-PRO3 fluorescent dye (Invitrogen Corp.) for 10 min. During analysis, dead cells were gated out as the FL4-higher fraction. The cell surface VE-cadherin-positive and VE-cadherin-negative fractions were sorted using as FACSAria™ (BD Biosciences) after cells were stained VE-cadherin (clone TEA1/31)-phycoerythrin (PE) antibody (Beckman Coulter Inc.).

Immunostaining

The cells were fixed on slide glasses with a cytospin apparatus (Cytospin 2) with further fixation with acetone/methanol solution (1:3). The immunostaining procedure was performed as described elsewhere (Saeki et al., 2003) with first antibody reactions using a mouse anti-human VE-cadherin antibody (clone55-7H1) (BD Biosciences), a rabbit anti-human N-cadherin antibody (H-63) (Santa Cruz Biotechnology Inc., Santa Cruz, CA), a rabbit polyclonal anti-human Nanog antibody (ReproCELL Inc., Tokyo, Japan), a mouse monoclonal anti-human Actin, α smooth muscle (SMA) (clone 1A4) (Sigma Chemical Co.), a mouse monoclonal anti-platelet-derived growth factor receptor β (PDGF-Rβ (clone 28) (BD Biosciences), a rabbit polyclonal anti-human eNOS antibody (H-159) (Santa Cruz Biotechnology Inc.), a goat polyclonal anti-human vWF antibody (C-20) (Santa Cruz Biotechnology Inc.) or a mouse monoclonal anti-CD68 antibody (Transgenic Inc., Kobe, Japan) followed by second antibody reactions using Alexa Fluor® 488 chicken anti-mouse IgG (H + L), Alexa Fluor® 568 goat anti-rabbit IgG (H + L) or Alexa Fluor® 594 chicken anti-goat IgG (H + L) (Molecular Probes, Inc., Eugene, OR).

Cord formation assays

Matrigel (BD Biosciences) was loaded into the 24 multi-well dishes (95 μl/well). After the dishes were incubated for 30 min at 37°C, 1×10^4 cells per well were seeded in 1 ml of EGM®-2 BulletKit supplemented with cytokines and growth factors according to the manufacturer's instructions (Cambrex Bio Science Walkersville, Inc., Walkersville, MD). Cell morphologies were observed after overnight culture under an inverted light microscope (Olympus Optical Co. Ltd.).

Colony assays

Colony assays were performed using Methocult TM GF^+H4535 (Stemcell Technologies Inc., Vancouver, Canada) according to the manufacturer's recommendations. In brief, 0.3 ml of cell suspension, which contained 10 cells, was mixed in 3 ml of methylcellulose solution consisting of 1% methylcellulose, 30% FBS, 1% bovine serum albumin, 0.1 mM β-mercaptoethanol, 2 mM L-glutamine, 50 ng/ml SCF (Pepro Tech Inc.), 20 ng/ml IL-3 (Pepro Tech Inc.), 20 ng/ml IL-6 (Pepro Tech Inc.), 20 ng/ml granulocyte-macrophage colony-stimulating factor (GM-CSF; Pepro Tech Inc.), 20 ng/ml granulocyte colony-stimulating factor (G-CSF; Kirin Brewery Company, Ltd., Tokyo, Japan) and 3 U/ml erythropoietin (Kirin Brewery Company, Ltd.) in 3.5-cm culture dishes. After 2 weeks, the number of colonies was counted. The morphology of the colonies was observed under an inverted light microscope (Olympus Optical Co. Ltd.).

Western blotting

Western blotting was performed as described previously (Saeki et al., 2003) using a rabbit anti-human VE-cadherin antibody (C-19) (Santa Cruz Biotechnology Inc.) or a mouse monoclonal anti-tubulin β (D-10) antibody (Santa Cruz Biotechnology Inc.). The second antibody reaction was performed using a horseradish peroxidase-conjugated anti-rabbit or anti-mouse IgG (Cell Signaling Technology, Inc., Beverly, MA). The final detection procedure was performed using ECL Western blotting detection reagents (GE Healthcare UK Ltd., Buckinghamshire, England).

Uptake of acetylated low-density lipoprotein (Ac-LDL)

Cells were transferred in 4-well chamber slide system (Nalge Nunc International Corp., Naperville, IL). After overnight culture, cells were washed by Hank's balanced salt solution (HBSS) twice and incubated in serum-free medium containing 10 μg/ml of low-density lipoprotein from human plasma, acetylated, DiI complex (DiI Ac-LDL) (Molecular Probes) for 4 h. After washing the cells by HBSS for three times, the cells were observed under the fluorescence microscope (Olympus Optical Co. Ltd.).

Polymerase chain reaction (PCR)

Genomic PCR. Genomic DNA was extracted from ES-derived vascular endothelial cells (ESdEC), HUVECs (Cambrex Bio Science Walkersville, Inc.) or MEFs of the ICR stain (CLEA Japan, Inc., Tokyo, Japan). 1×10^6 cells were lysed with a buffer (50 mM Tris–HCl (pH 8.0), 0.1 M NaCl, 20 mM EDTA and 0.1% SDS) supplemented with 75 μg/ml Proteinase K (WAKO Pure Chemical Industries, Osaka, Japan) for 8 h at 55°C. After phenol/chloroform extraction and isopropanol precipitation, dried pellets were solubilized by 100 μl of water containing 50 ng/ml DNase-free RNase (Invitrogen Corp.) and incubated for 1 h at 37°C. The genomic DNA solution was kept at −80°C. PCR was performed using 2 μl of the 50× diluted DNA template, SP-Taq (Hokkaido System Science Co., Ltd., Hokkaido Japan) and following primers. For detecting the murine ly 9.2 genomic fragment, a forward primer 5′-gtaaattcccccagccctgt-3′ and a reverse primer 5′-atgccatgtcctcttcatccs-3′ were used (the product length is 433 bp). For detecting the primate CD34 genomic fragment, a forward primer 5′-CGACAGTCAAATTCACATCTACC-3′ and a reverse primer 5′-GAGATGTTGCAAGGCTAGTGC -3′ were used (the product length is 254 bp). The PCR procedure was carried out using a DNA Thermal Cycler PJ2000 (PerkinElmer Corp., Foster City, CA) with the following program: 95°C; 5 min, 94°C; 30 sec, 57°C; 30 sec, 72°C; 1 min at 27 cycles for murine ly9.2 and at 34 cycles for primate CD34. The product was separated by agarose gel electrophoresis and the DNA was visualized by ethidium bromide staining. A 100 bp ladder marker 4 (Nippon Gene Co. Ltd., Tokyo, Japan) was used to evaluate the molecular weights of the PCR products.

Reverse transcription-polymerase chain reaction (RT-PCR). RNA was extracted from 5×10^6 cells with RNeasy Mini Kit (Qiagen Inc., Valencia, CA) and cDNA was synthesized by Superscript II Kit (Invitrogen Corp.) according to a manufacture's protocol. The PCR procedure was carried out as described above using primate globin-ε primers; a forward primer 5′-TGCATTTTACTGCTGAGGAGA-3′ and a reverse primer 5′- AAGAGAACTCAGTGGTACTT-3′, primate globin-ζ primers; a forward primer 5′-TTCCTCAGCCACCCGCAGAC-3′ and a reverse

primer 5′-AGCAGGCAGTGGGACAGGAG-3′, primate VE-cadherin primers; a forward primer 5′-TGGGCTCAGACATCCACATA-3′ and a reverse primer 5′-TCACAGTCTCCCTTGGGAAT-3′. For internal control, primate β-actin primers were used: a forward primer 5′-gCAggAgATggCCACggCgCC-3′ and a reverse primer 5′-TCTCCTTCTgCATCCTgTCggC-3′.

Collagen plug assay

About 10 blocks of dried honeycomb collagen sponge (Koken Co. Ltd., Tokyo, Japan) were mixed with 500 μl of cmES-derived cells at passage number 4, which were suspended in differentiation medium at the density of 4×10^5/ml, and were then cultured for 2 days in vitro. Then they were transplanted intraperitoneally into SCID mice. After 35 days, 0.2 ml of FITC-dextran (500,000 average molecular size, Sigma Chemical Co.) solution (100 mg FITC-dextran suspended in 5 ml PBS) was injected into mice from a tail vein. After several minutes, mice were sacrificed and the blocks were fixed by 10% formaldehyde and paraffin embedded. The 4 μm sliced specimen were further subjected to immunostaining using a mouse monoclonal anti-human HLA-A, B, C antibody (BD Biosciences) or a rabbit polyclonal anti-PECAM-1 antibody (H-300) (Santa Cruz Biotechnology Inc.), and also to histological examination using hematoxylin and eosin solutions.

Results

A sac-like structure with surrounding cobblestone cells as a parental organization for vascular endothelial cell generation

During our attempt to generate hematopoietic progenitor cells from cmES cells under feeder-free conditions, we found that the condition we had tried to optimize for hematopoietic differentiation was unexpectedly fitted for the production of vascular endothelial cells. Our differentiation medium was prepared by modifying the one reported in a case of hematopoietic differentiation of rmES cells by co-culture method (Li et al., 2001). In the presence of VEGF, BMP-4, SCF, Flt3-L, IL-3, IL-6 and serum, we generated spheres from cmES cells (Fig. 1A,B, upper left). Then spheres were subjected to adherent culture on gelatin-coated dishes (Fig. 1A,B, upper middle and right). Time course observations revealed the differentiation processes as follows: spreading of cobblestone-shaped cells with leaving the center region rather amorphous in a few days (Fig. 1B, lower left); swelling of the center region at about 6 days (Fig. 1B, lower middle); ballooning out of the center region resulting in the formation of "a sac-like structure" filled with abundant round cells, some of which brimmed over the sac wall, around 12 days (Fig. 1B, lower right). At this time, the cobblestone cells were divided into two populations by their morphology. The cells located at proximal regions to the sac-like structure became densely packed, while the cells located at distal regions remained rather stretched (Fig. 1C). Although the early phased cobblestone cells (Fig. 1B, lower left) did not express VE-cadherin but expressed only N-cadherin at intercellular junctions (data not shown), VE-cadherin expression had become detectable in all adherent cells at the time when a sac-like structure was formed. As shown in Figure 1D, the late phased cobblestone cells, including proximal compact cells and distal extended cells, as well as sac wall cells expressed VE-cadherin at intercellular junctions. Thus, total adherent cells generated after the culture of ES-derived spheres on gelatin-coated dishes using our differentiation medium are regarded as vascular endothelial cell-committed populations although no special selection procedures were performed.

We also studied the characteristics of the non-adherent round cells, majority of which located within the sacs and minor portion of which resided around the sacs. They were collected from the culture supernatant after cutting the sac walls by micropipettes and releasing into the medium. The cytochemical analysis including Wright-Giemsa, myeloperoxidase and esterase staining showed that the majority of the round cells were myeloblasts and macrophages (Fig. 1E). This finding was further supported by the results of colony assays of round cells, where generation of granulocyte/macrophage colonies consisting of promyelocytes, myelocytes, and segmented neutrophils were observed (Fig. 1F). Because sac-like structures resembled the morphology of blood islands in the yolk sac, we investigated the possible existence of primitive hematopoietic cells. The RT-PCR studies showed that the messages for embryonic hemoglobins, globin-ε and globin-ζ, were expressed at the sac stage (Fig. 1G, lane 2 (cmES-derived cells, p1)) and subsequent first-passage-stage (Fig. 1G, lane 3 (cmES-derived cells, p2)). Thus, non-adherent round cells consist of myeloblasts and macrophages along with a small portion of primitive erythroid cells.

Hence, simple adherent culture of ES-derived spheres in the presence of hematopoietic cytokines resulted in generation of a unique construction: a sac-like structure and surrounding cobblestone cells that expressed VE-cadherin along with primitive and definitive hematopoietic cells localized within and around the sac.

Characterization of subcultured adherent cells

We next tried to expand the cell surface VE-cadherin-positive adherent cells by an ordinary subculture method. After cutting sac walls and releasing the inner hematopoietic cells into culture supernatant, residual adherent cell populations including sac wall-constituting cells and surrounding cobblestone cells were detached by trypsin/EDTA treatment and transferred massively onto new gelatin-coated dishes. During the cutting process of the sac walls, they were divided into small fragments but remained attached to dishes. After trypsin/EDTA treatment, the cells were dissociated almost into single cell and transferred to new gelatin-coated plates by 1:3 dilution. Cells actively proliferated and reached confluence in 3–4 days. They showed highly homogenous spindle-shaped morphology similar to HUVEC (Fig. 2A). Indeed, these cmES-derived cells showed cord-forming activities equivalent to HUVEC (Fig. 2B). Furthermore, all of the cells were positive for Ac-LDL-uptaking activities (Fig. 2C) with uniform expressions of eNOS and vWF (described in the following part of the manuscript and Fig. 4B, left parts).

To quantitatively evaluate the vascular endothelial differentiation, we determined the cell surface expression of VE-cadherin and PECAM-1 by flow cytometry. As shown in Figure 3A, limited populations were positive for VE-cadherin and PECAM-1 despite rather uniform expression of VE-cadherin before subculture (Fig. 1D). Although the reason for the reduction of VE-cadherin expression after subculture was not known, the expressions of VE-cadherin/PECAM-1 were well preserved during subsequent culture (Fig. 3B). The cells were subculturable up to eight passages, during which 2×10^5 cmES cells generated 7×10^9 of VE-cadherin/PECAM-1-positive vascular endothelial cells. Moreover, the cells were freeze–thaw-tolerable and re-cultured cells properly retained the VE-cadherin/PECAM-1 expressions (Fig. 3C). The average percents of VE-cadherin/PECAM-1-positive cells were $29.8 \pm 15.1\%$ ($n = 17$). The expressions of other surface markers for vascular endothelial cells were also examined. As shown in Figure 3D, the expression of VEGF-R1, a vascular endothelial cell-specific marker, was detected at a comparable level to HUVEC and HAEC. Tie-2 expression was also detected in cmES-derived cells although the expression levels were slightly lower than HUVEC and HAEC. On the other hand, CD34-positive populations were detected mainly in cmES-derived cells and HUVEC. Interestingly, the expression of

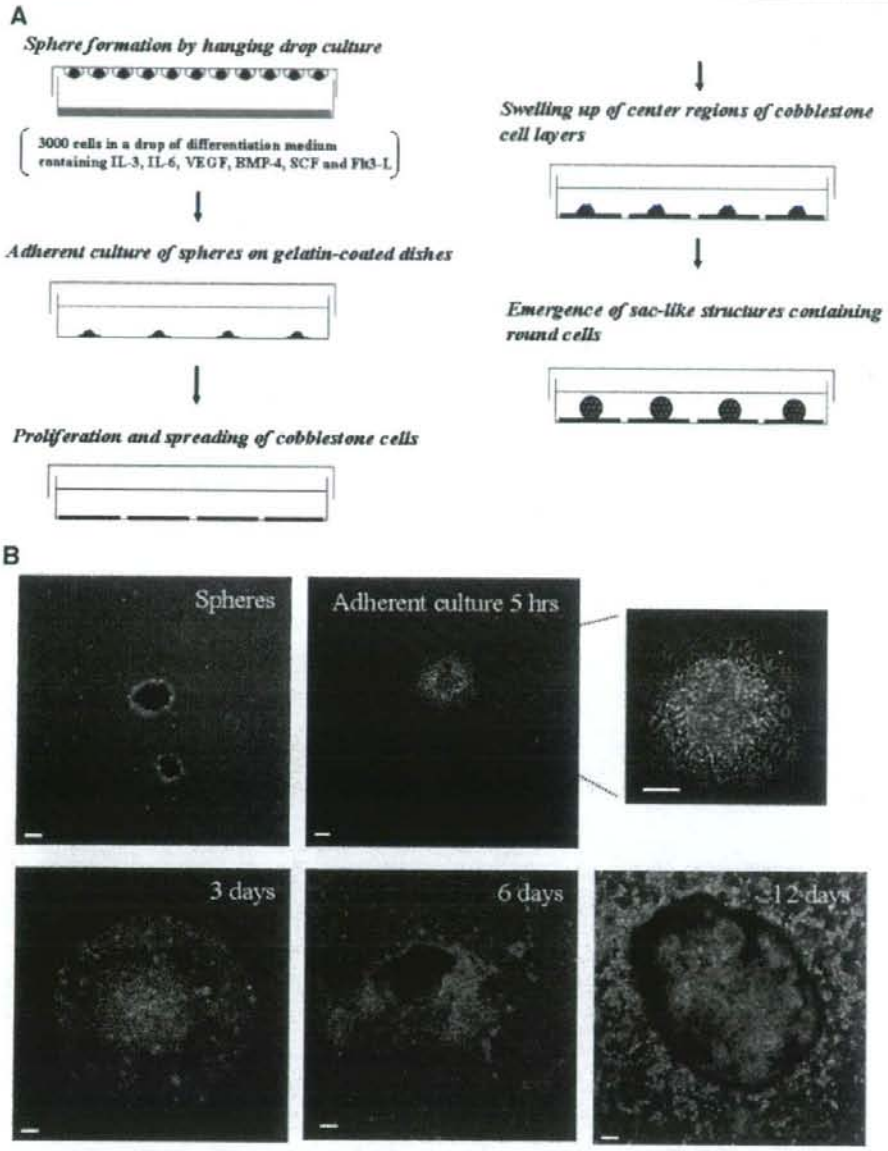

Fig. 1. Generation of a sac-like structure and cobblestone cells from feeder-free differentiation culture of cmES cells. The procedure for the production of a sac-like structure (A) and phase contrast microscopy (B). Spheres were generated by a hanging drop culture and subjected to subsequent adherent culture using gelatin-coated plates. Within a few days, spheres adhered on the plates became flattened and VE-cadherin-negative cobblestone cells spread out. At about 6 days, the center region began to swell up again. Around 12 days, the center regions ballooned out and sac-like structures were formed. Scale bars indicate 100 μm. C: The phase contrast microscopy of late phase cobblestone cells. Morphologies of proximal and distal cobblestone cells that surrounded a sac-like structure were shown. The scale bar indicates 100 μm. D: VE-cadherin expression in late phase cobblestone cells. Sac-like structure and surrounding cobblestone cells were stained with anti-VE-cadherin antibody. The scale bar indicates 50 μm. E: Morphological and cytochemical examinations of the round cells released from the sac-like structure. The Wright-Giemsa staining (WG) showed the presence of two types of the cells: the small cells with basophilic cytoplasm and high nucleus/cytoplasm ratio resembling myeloblasts and the large cells with abundant vacuolated cytoplasms resembling macrophages. The myeloperoxidase staining (MPO) showed that majority of the small cells were positive for myeloperoxidase. The esterase double staining (Esterase) showed the cells with blue granules (granulocyte lineage cells) and cells with brown granules (macrophage lineage cells). The scale bar indicates 100 μm. F: Hematopoietic colony assays. The round cells released from the sac-like structure were subjected to hematopoietic colony assays. The phase contrast microscopic observation (Phase) showed the presence of granulocyte/macrophage colonies. Wright-Giemsa staining (WG) of the cells from colonies showed the presence of myeloblasts (a black arrow), promyelocytes (a blue arrow) and polymorphonuclear granulocytes (a red arrow). The myeloperoxidase staining (MPO) showed the presence of a myeloperoxidase-rich smaller granulocyte population (a black arrow) and a myeloperoxidase-poor large macrophage population (a red arrow). Esterase double staining (Esterase) showed the presence of cells with blue granules (a black arrow) and cells with brown granules (a red arrow). The scale bar indicates 100 μm. G: RT-PCR. The presence of primitive hematopoietic cells was shown by the existence of messages for embryonic hemoglobins (globin-ε and globin-ζ) using primate-specific primers (pr-globin-ε, pr-globin-ζ, and pr-β-actin). "M" indicates 100 bp ladder marker. The subscript character of "p" of cmES-derived cells indicates the passage number. "H"; HUEVC, "E"; undifferentiated cmES cells, "U"; hematopoietic UT-7 cells as positive control. [Color figure can be viewed in the online issue, which is available at www.interscience.wiley.com.]

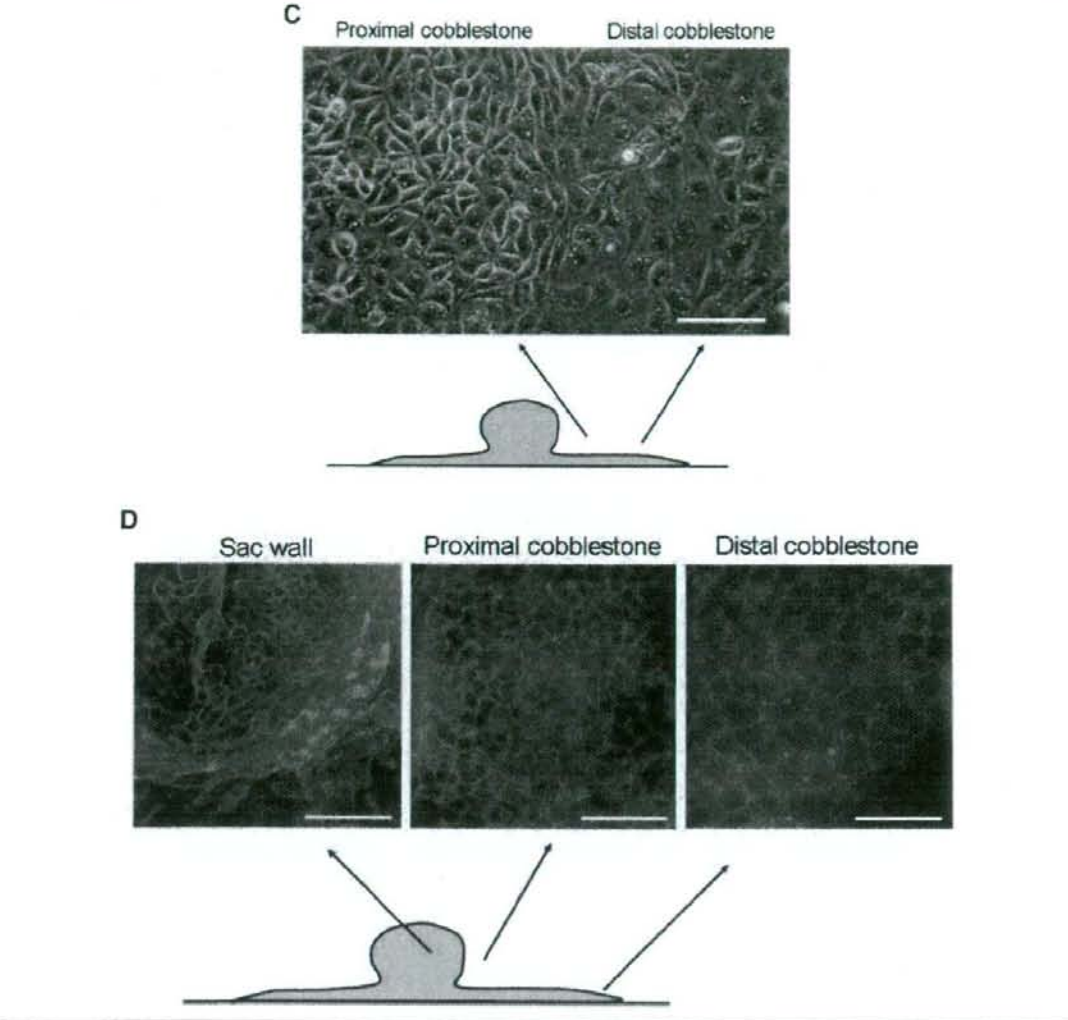

Fig. 1. (*Continued*)

VEGF-R3, a marker for lymphatic endothelial and embryonic vascular endothelial cells, was detected at fairly high levels in cmES-derived cells and HUVEC. The expression of VEGF-R2, a marker for vascular and lymphatic endothelial cells, was constantly detected at the same level as VE-cadherin, as we confirm it by detailed analyses in the following part of the manuscript (Fig. 5). From these flow cytometric analyses, it was concluded that cmES-derived cells resembled HUVEC rather than HAEC.

Although limited populations of cmES-derived cells were positive for cell surface VE-cadherin/PECAM-1, their uniform Ac-LDL-uptaking activities and uniform expressions of eNOS and vWF, taken together with their cord-forming activities and VEGF-R1 expression equivalent to HUVEC, suggest that the almost all of the cmES-derived cells are vascular endothelial cells or vascular endothelial endothelial-like cells and, therefore, "VE-cadherin/PECAM-1-negative" populations are also types of cells that are closely related to the vascular endothelial cells. This idea was analogous to the proposal by Thomson and colleagues (Kaufman et al., 2004). They showed that rmES-derived vascular endothelial cells were negative for VE-cadherin/PECAM-1 despite the presence of mature endothelial functions with eNOS and vWF expressions. They used commercially available EGM®-2 BulletKit for the differentiation of rmES cells. Eventually, usage of EGM®-2 BulletKit resulted in the production of almost pure VE-cadherin/PECAM-1-negative vascular endothelial cells by our method as the report by Thomson and colleagues. As shown in Figure 4, differentiation induction by our method using EGM®-2 BulletKit resulted in generation of cells with mature

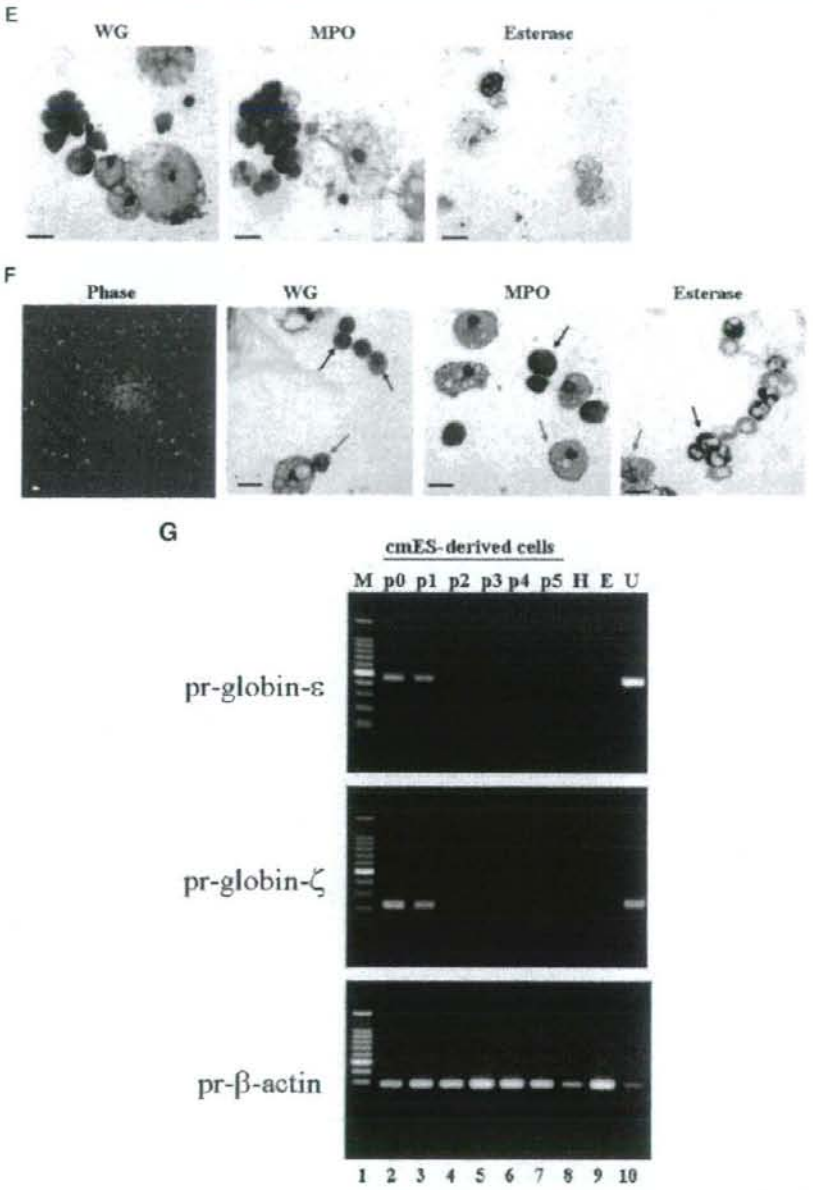

Fig. 1. (*Continued*)

functions including cord-forming activities (Fig. 4A, upper right in EGM2 part) and uniform Ac-LDL-uptaking activities (Fig. 4A, middle and lower right in EGM2 part) and with eNOS and vWF expressions (Fig. 4B, EGM2 part) despite the lack of VE-cadherin/PECAM-1 as assessed by flow cytometry (Fig. 4A, lower left in EGM2 part). In contrast to the findings by Thomson and colleagues (Kaufman et al., 2004), VE-cadherin expression was detected by Western blotting (Fig. 4C) in our culture system even by using EGM®-2 BulletKit, indicating that VE-cadherin protein was really produced though its membrane translocation seems to be blocked by unknown reason(s). Anyway, it can be concluded that there existed an "atypical"

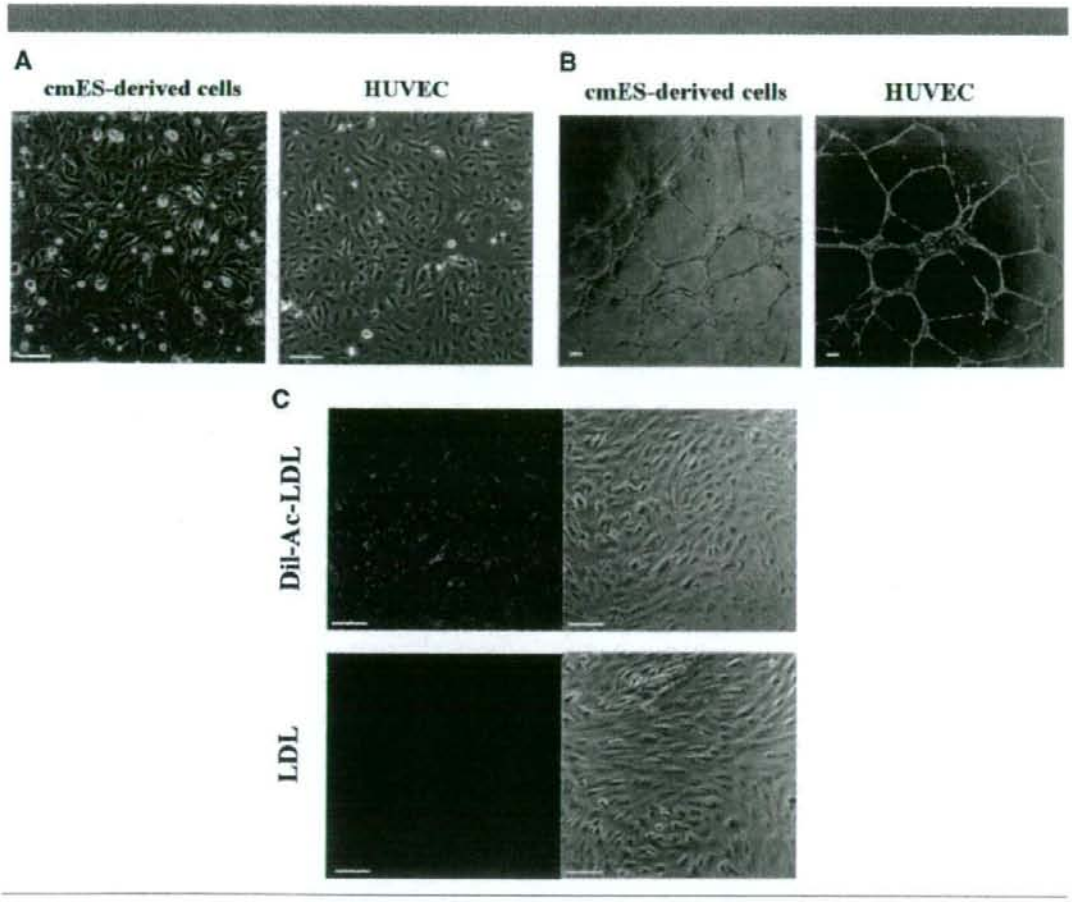

Fig. 2. Morphology and functions of cmES-derived subcultured cells. A: The phase contrast microscopy. Morphologies of cmES-derived cells (left) and HUVEC (right) were shown. The scale bar indicates 100 μm. B: Cord formation assays. A cord-forming activity of cmES-derived cells (left) and HUVEC (right) was shown. The scale bar indicates 100 μm. C: Ac-LDL-uptaking assays. Fluorescence (DiI)-labeled Ac-LDL (upper) or non-labeled LDL (lower) was added to cmES-derived cells. After overnight culture, cells were observed under fluorescence microscopy. Right parts indicate the photographs with Normarsky differentiated interference contrast. The scale bar indicates 20 μm.

type of vascular endothelial cells (i.e., cell surface VE-cadherin/PECAM-1-negative vascular endothelial cells) among primate ES-derived differentiated cells.

For further understanding of cell surface VE-cadherin-positive "canonical" vascular endothelial cells and cell surface VE-cadherin-negative "atypical" vascular endothelial cells, we fractionated those two populations by FACSAria. As shown in Figure 5C, cell surface VE-cadherin-positive populations proliferated as VE-cadherin-positive cells and expanded by 160-fold after five passages. Interestingly, cell surface VE-cadherin-positive populations were positive for cell surface CD34 expression as assessed by flow cytometry (Fig. 5D). The immunostaining study of cell surface VE-cadherin-positive cells clearly showed the localization of VE-cadherin at intercellular junctions in these cells (Fig. 5E). The functional maturation including cord-forming activities (Fig. 5F) and uniform Ac-LDL-uptaking activities (Fig. 5G) was also detected in cell surface VE-cadherin-positive populations. Expressions of other vascular endothelial markers were also detected including VEGF-R1, VEGF-R2, VEGF-R3, and Tie-2 (Fig. 5H). On the other hand, the cell surface VE-cadherin-negative populations proliferated as VE-cadherin-negative cells and were negative for cell surface CD34 expression (Fig. 6A–D). Interestingly, these cells showed obvious cord-forming capacities (Fig. 6E) and a uniform Ac-LDL-uptaking activity (Fig. 6F). Moreover, they expressed VEGF-R1, VEGF-R3, and Tie-2 despite the absence of VEGF-R2 as demonstrated by flow cytometric analyses (Fig. 6G). Immunostaining studies using an anti-VE-cadherin antibody demonstrated intracellular region-staining patterns (Fig. 6H), suggesting that the cell surface VE-cadherin-negative cells expressed VE-cadherin intracellularily. This finding was confirmed by Western blotting studies, which showed the presence of the 130-kDa VE-cadherin band (Fig. 6I). RT-PCR studies further demonstrated the presence of the VE-cadherin message (Fig. 6J). As monocytes/macrophages or other hematopoietic cells reportedly show various endothelial cell-like features and are positive for VEGF-R1 and VEGF-R3

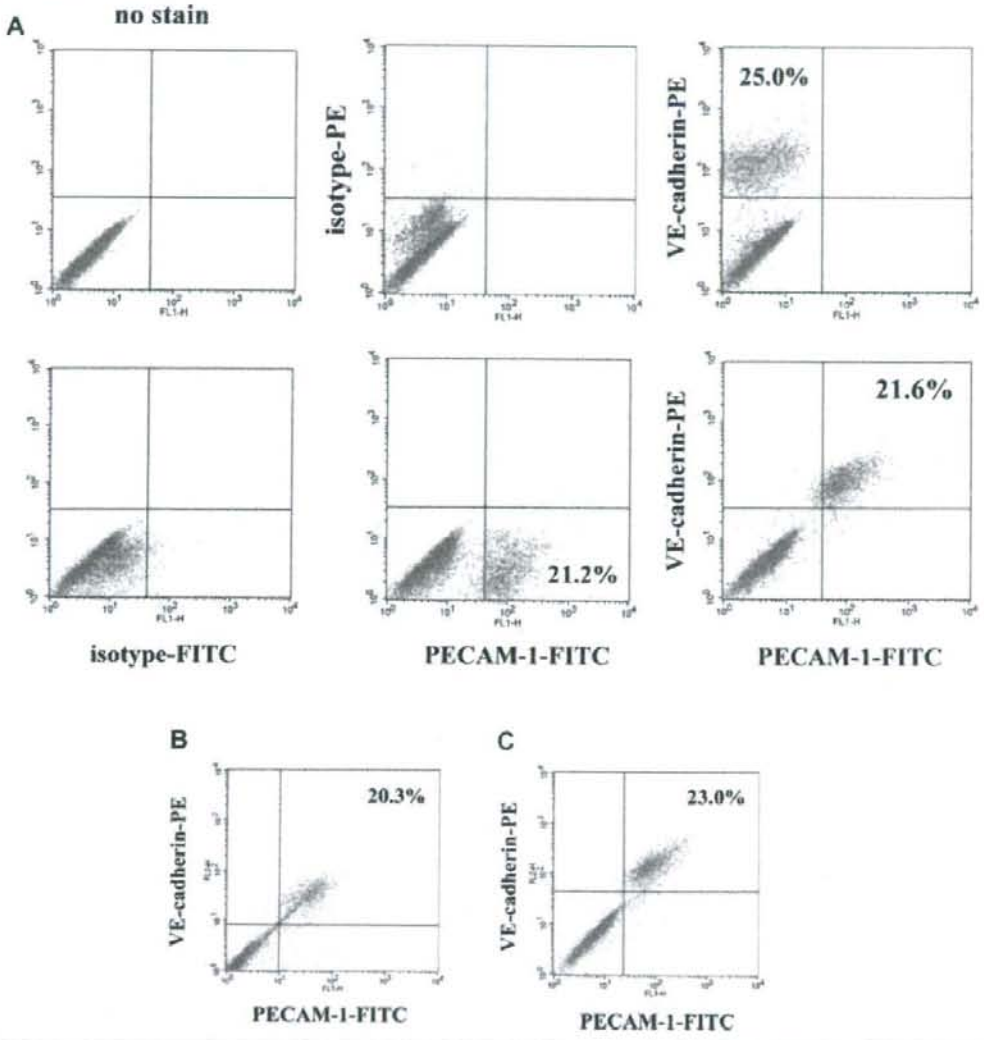

Fig. 3. Cell surface expressions of vascular endothelial markers in cmES-derived subcultured cells. A–C: Cell surface expressions of VE-cadherin and PECAM-1. The total adherent cells obtained by culture of cmES-derived spheres on gelatin-coated plates were subcultured and, after six passages (A) or eight passages (B), cells were stained by a PE-labeled anti-human VE-cadherin antibody (vertical axes), a FITC-labeled anti-human PECAM-1 antibody (horizontal axes) or each isotype control antibody as indicated. C: The total adherent cells obtained by the culture of cmES-derived spheres on gelatin-coated plates were frozen. After being thawed, cells were cultured for additional two passages and the expressions of VE-cadherin and PECAM-1 were determined by flow cytometry as in (A). D: Expressions of other endothelial markers. cmES-derived cells (ESdC), HUVEC and HAEC were subjected to flow cytometric analyses using indicated monoclonal antibodies.

(Fernandez Pujol et al., 2001; Kuwana et al., 2006), we examined the expressions of monocyte/macrophage markers of CD68, CD14 and CD11b as well as pan-leukocyte markers of CD18 and CD45. We found that the cell surface VE-cadherin-negative populations were negative for CD68 (Fig. 6K), CD14 (Fig. 6L), CD11b (Fig. 6L), CD18 (Fig. 6L), and CD45 (Fig. 6L), indicating that they are distinct from hematopoietic endothelial cell progenitors.

All those findings together suggest that our differentiation system produced almost two pure populations: cell surface VE-cadherin-positive "canonical" vascular endothelial cells and cell surface VE-cadherin-negative "atypical" vascular endothelial cells. This concept was further confirmed by the fact that neither pericytes nor undifferentiated ES cells co-existed in the differentiated samples. Pericytes are reportedly induced during vascular endothelial differentiation (Yamashita et al., 2000; Sone et al., 2003, 2007). Moreover, co-existence of pericytes, the polygonal cells, severely inhibits the expansion of vascular endothelial cells during subculture (Sone et al., 2003, 2007). In our system, however, both

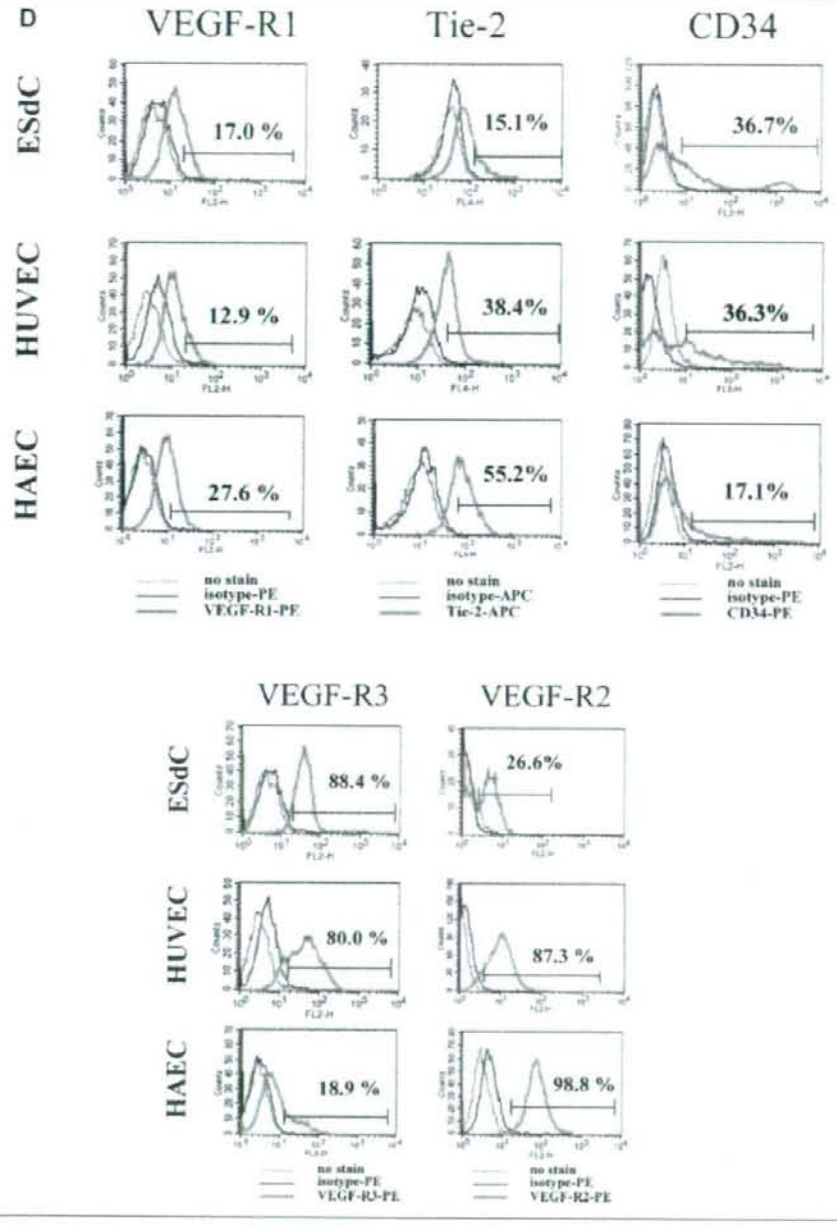

Fig. 3. *(Continued)*

VE-cadherin-positive and VE-cadherin-negative populations showed quite similar spindle-shaped morphologies (but not polygonal shape) and were undistinguishable by microscopic observations (Figs. 5B and 6B). Indeed, our differentiated samples were negative for the expressions of smooth muscle actin (SMA)-α, a marker for smooth muscle cells, and PDGF receptor β, a marker for pericytes (Fig. 7A). As shown in Figure 7B,C, Nanog expression was not detected in ES-derived cells, excluding the possible existence of undifferentiated ES cells. Finally, genomic PCR studies excluded the contamination of MEFs, which were used only in the maintenance culture of undifferentiated cmES cells (Fig. 7D).

Thus, our novel method has enabled the highest efficiency vascular endothelial differentiation from primate ES cells,

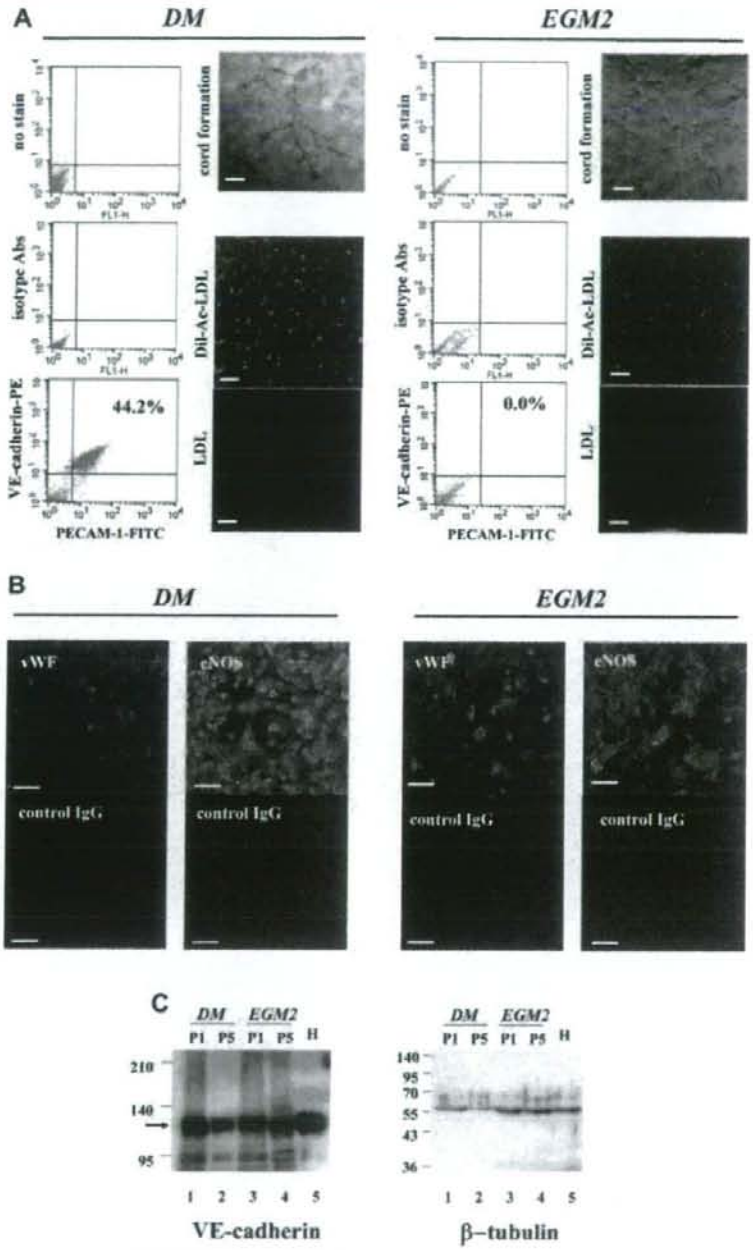

Fig. 4. Generation of atypical vascular endothelial cells by using commercially available culture medium. Differentiation procedure was performed either by using the differentiation medium supplemented with six cytokines (*DM*) or EGM®-2 BulletKit medium (*EGM2*). A: After two passages, flow cytometric analyses for cell surface VE-cadherin/PECAM-1 expressions (left parts), cord formation assays (right upper parts) and Ac-LDL uptaking assays (right lower parts) were performed in each culture condition (DM culture or EGM2 culture). The scale bar indicates 100 μm. B: After two passages, cells were fixed and stained by an anti-human vWF goat polyclonal antibody (red) and an anti-human eNOS rabbit polyclonal antibody (green). The scale bar indicates 50 μm. Similar results were obtained at passage number at least up to 7 (data not shown). C: At indicated numbers of passage, cells were collected and Western blotting was performed using an anti-human VE-cadherin rabbit polyclonal antibody. Arrows indicate the 130 kDa VE-cadherin protein (left part). For positive control, HUVEC lysate was used (lane 5, "H"). For internal control, β-tubulin expressions were determined (right part).

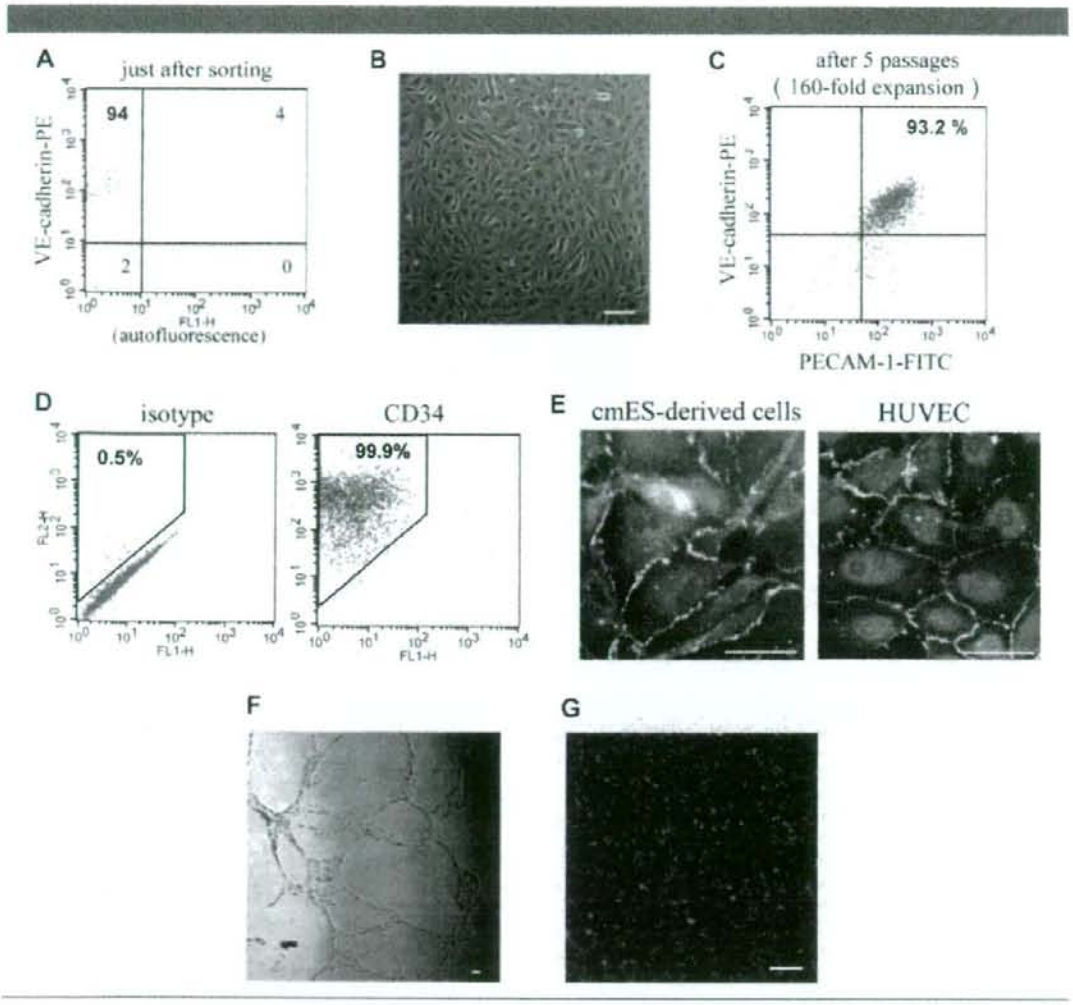

Fig. 5. Expansion and characterization of cell surface VE-cadherin-positive populations. Differentiation procedure was performed, and after the first passage, cell surface VE-cadherin-positive fraction was sorted by FACSAria™. A: The expression of VE-cadherin was determined just after sorting. B: After a few days culture, cell morphology was observed under an inverted phase contrast light microscope. The scale bar indicates 100 μm. C: After five passages, the cell surface expressions of VE-cadherin/PECAM-1 were re-studied by flow cytometry. D: The cell surface expression of CD34 was also studied by flow cytometry. E: Localization of VE-cadherin at intercellular junctions was confirmed by immunostaining using HUVEC as positive control. The scale bar indicates 50 μm. F,G: The functional analyses. Cord-forming activities (F) and Ac-LDL-uptaking capacities (G) were confirmed. The scale bar indicates 100 μm. H: Cell surface expressions of other endothelial markers (VEGF-R2, VEGF-R1, VEGF-R3, and Tie-2) were studied by flow cytometry.

providing pure production of vascular endothelial cells including VE-cadherin-negative "atypical" vascular endothelial cells.

The in vivo functions of ES-derived vascular endothelial cells

We next studied the in vivo functions of cmES-derived vascular endothelial cells by performing collagen sponge plug assays. Honeycomb collagen sponges were mixed with cmES-derived vascular endothelial cells (at passage 3) and transplanted intraperitoneally into SCID mice. After 35 days, FITC-dextran was injected from tail vein and then plugs were excited and histologically examined. As shown in Figure 8A, multiple FITC-dextran-filled lumens were detected in the collagen plugs, indicating the presence of neovascularization connected with systematic circulation within the plugs. Histological observations further confirmed the presence of neovascularization, which was filled with erythrocytes (Fig. 8B). The cells that lined the neovascular lumens as well as the cells remaining within the honeycomb plugs were all stained by both an anti-human HLA-A, B, C antibody (Fig. 8C, left middle part), which distinguishes primate cells from murine cells (Kaufman et al., 2004), and by an anti-human PECAM-1 antibody (Fig. 8C, right middle parts) which shows their endothelial nature. Finally, these vascular structures with human (primate)

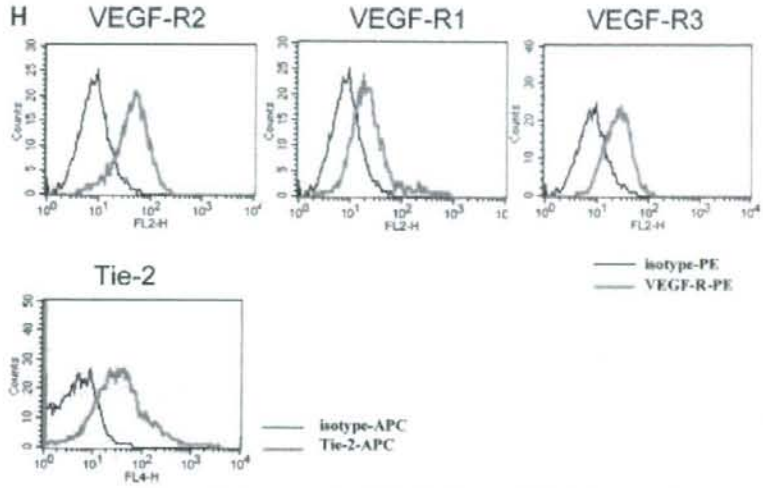

Fig. 5. *(Continued)*

HLA and PECAM-1 were again shown to be connected with systematic circulation (Fig. 8C, lower left and right parts).

Thus, the cmES-derived vascular endothelial cells produced by our method are functional in vivo.

Evaluation of the roles of each medium component for effective differentiation

Finally, we re-evaluated the requirement of each component of our differentiation medium for vascular endothelial differentiation of cmES cells. First we studied the necessity of each cytokine for the generation of spheres, sac-like structures and cell surface VE-cadherin/PECAM-1-positive cells by checking the effects of depletion of each one cytokine from differentiation medium.

Depletion of IL-3 or IL-6 deteriorated the quality of spheres: the spheres often failed to proliferate during subsequent adherent culture (data not shown). In regard to the other four cytokines (BMP-4, SCF, Flt3-L, and VEGF), depletion of BMP-4 resulted in the formation of sac-like structures with poor hematopoiesis (Fig. 9A). On the other hand, depletion of SCF, Flt3-L and VEGF did not affect the formation of sac-like structures (Fig. 9A).

When estimated by the performance for the induction of cell surface VE-cadherin/PECAM-1-positive cells, all of the four cytokines BMP-4, SCF, Flt3-L and VEGF were found to play important roles in differentiation. Depletion of BMP-4, SCF, or Flt3-L deteriorated the performance levels in producing cell surface VE-cadherin/PECAM-1-positive cells (Fig. 9C,D). Although in some cases, depletion of each cytokine did not dramatically reduce the percentages of cell surface VE-cadherin/PECAM-1-positive cells (Fig. 9C), it did abolish the generation of cell surface VE-cadherin/PECAM-1-positive cells in other cases (Fig. 9B). Approximately estimated, one out of three experiments, we failed in generation of cell surface VE-cadherin/PECAM-1-double-positive cells when BMP-4, SCF, or Flt3-L was depleted from the medium. Depletion of VEGF reproducibly reduced the percentages of cell surface VE-cadherin/PECAM-1-positive cells (Fig. 9B,C). In contrast, replacement of IMDM by RPMI 1640 medium did not affect the all processes of differentiation (Fig. 9A–C). On the other hand, no sac-like structures were generated by EGM®-2 BulletKit cultures even when supplemented with six cytokines or six cytokines plus 10% FBS (Fig. 9A). In addition, percentages of cell surface VE-cadherin/PECAM-1-positive cells were considerably low (Fig. 9B–C), a finding almost identical to EGM®-2 BulletKit culture without six cytokines (Fig. 4A, EGM part).

Thus, it was concluded that (1) IL-3 and IL-6 contribute to the improvement of the quality of spheres, (2) BMP-4 is essential for a sac-dependent hematopoiesis, (3) VEGF is critical for the production of cell surface VE-cadherin/PECAM-1-positive cells, (4) BMP-4, SCF and Flt3-L contribute to the stable induction of cell surface VE-cadherin/PECAM-1-positive cells, and (5) Differentiation medium can be prepared by using RPMI 1640 in place of IMDM, but not by using EGM®-2 BulletKit, for the production of a sac-like structure and cell surface VE-cadherin/PECAM-1-positive cells.

Discussion

In this article, we reported a method for high efficiency differentiation of vascular endothelial cells from feeder-free primate ES cells. cmES-derived vascular endothelial cells are subculturable and freeze–thaw-tolerable. An additional merit of our system is its feasibility: it does not require a process to sort the progenitor populations such as VEGF-R2-positive (Sone et al., 2003, 2007) or CD34-positive (Wang et al., 2007) fractions. To our knowledge, this is the highest efficiency system for the production of vascular endothelial cells. Indeed, our system provides almost two pure populations: the cell surface VE-cadherin/PECAM-1-positive "canonical" vascular endothelial cells and cell surface VE-cadherin/PECAM-1-negative "atypical" vascular endothelial cells. Co-existence of pericytes was excluded. Contamination of immature Nanog-expressing ES cells was also excluded. Eventually, no tumor formation was observed after transplanting the cmES-derived vascular endothelial cells into SCID mice (data not shown), encouraging a safe application of

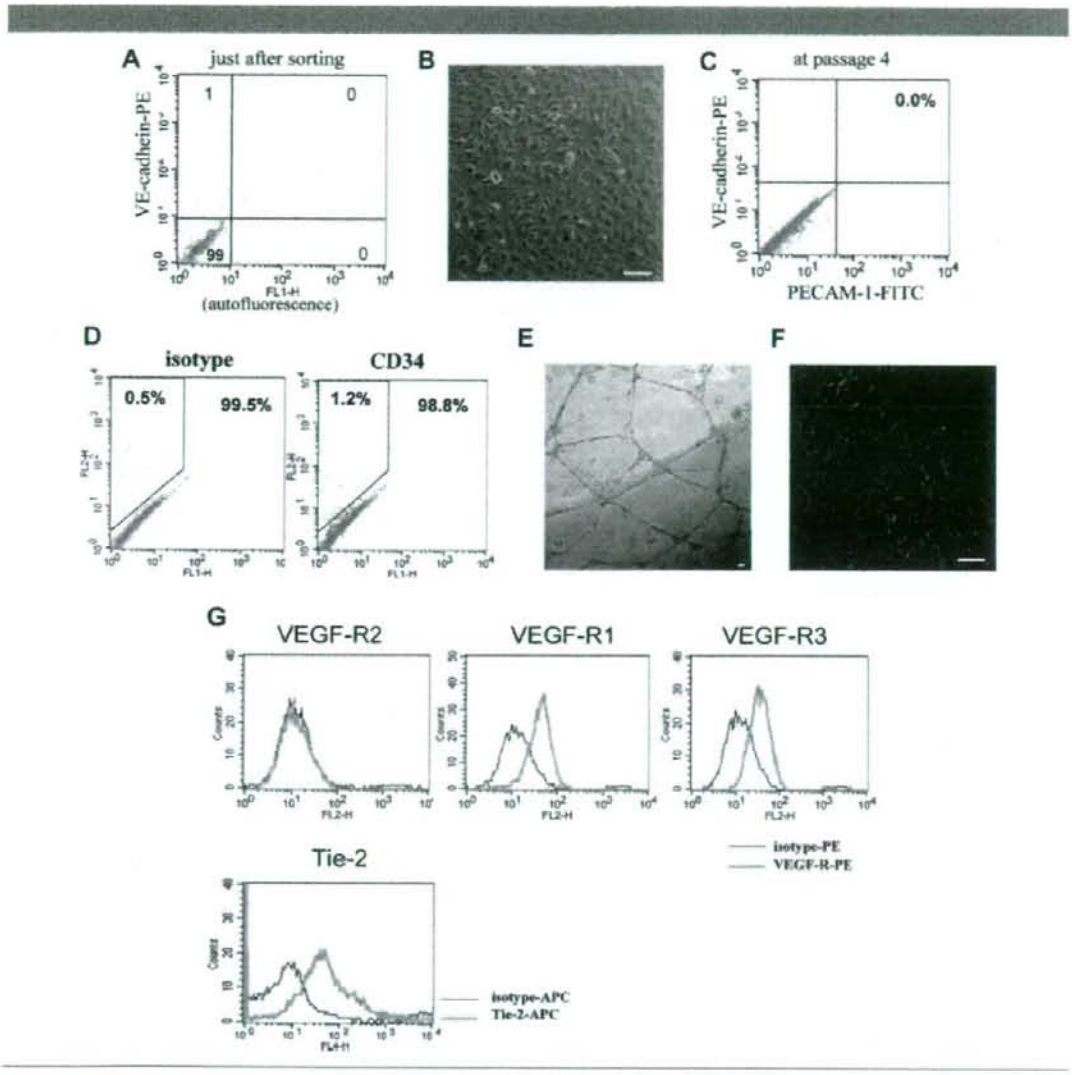

Fig. 6. Expansion and characterization of cell surface VE-cadherin-negative populations. Differentiation procedure was performed, and after the first passage, cell surface VE-cadherin-negative fraction was sorted by FACSAria™. A: The expression of VE-cadherin was determined just after sorting. B: After a few days culture, cell morphology was observed under an inverted phase contrast light microscope. The scale bar indicates 100 μm. C: After four passages, the cell surface expressions of VE-cadherin/PECAM-1 were re-studied by flow cytometry. D: The cell surface expression of CD34 was also studied by flow cytometry. E,F: The functional analyses. Cord-forming activities (E) and Ac-LDL-uptaking capacities (F) were confirmed. The scale bar indicates 100 μm. G: Cell surface expressions of other endothelial markers (VEGF-R2, VEGF-R1, VEGF-R3, and Tie-2) were studied by flow cytometry. H: VE-cadherin expression was determined by immunostaining studies. The cells were stained by an anti-VE-cadherin antibody (upper) or isotype control antibody (lower). The right parts indicate the phase contrast microscopy. The scale bar indicates 50 μm. I: Western blotting of VE-cadherin (left) and β-tubulin (right) of the cell surface VE-cadherin-negative population (lane 1) and the total population before sorting (lane 2). The expression of 130-kDa VE-cadherin band (indicated by arrow) was detected even in the cell surface VE-cadherin-negative population, indicating the intracellular localization of VE-cadherin. J: RT-PCR studies for VE-cadherin (upper) and β-actin (lower) were shown. The templates used were as follows: lane 1; cDNA of the cell surface VE-cadherin-negative population, lane 2; cDNA of total populations before sorting, lane 3; cDNA of HUVEC, lane 4; water, lane 5; cDNA of hematopoietic HL-60 cells. K,L: Immunostaining studies and flow cytometric analyses of hematopoietic and monocyte/macrophage markers. K: Cells were stained by an isotype control antibody (left) or an anti-CD68 antibody (right). Lower parts indicate the photographs with Normarsky differentiated interference contrast. The scale bar indicates 100 μm. L: Cell surface expressions of CD14 (upper, a bold green line), CD18 (middle, a bold green line), CD11b (lower, a bold green line), and CD45 (lower, a bold pink line) were studied. Thin black lines indicate the data of non-staining samples and bold black lines indicate the data of isotype control antibody-stained samples.

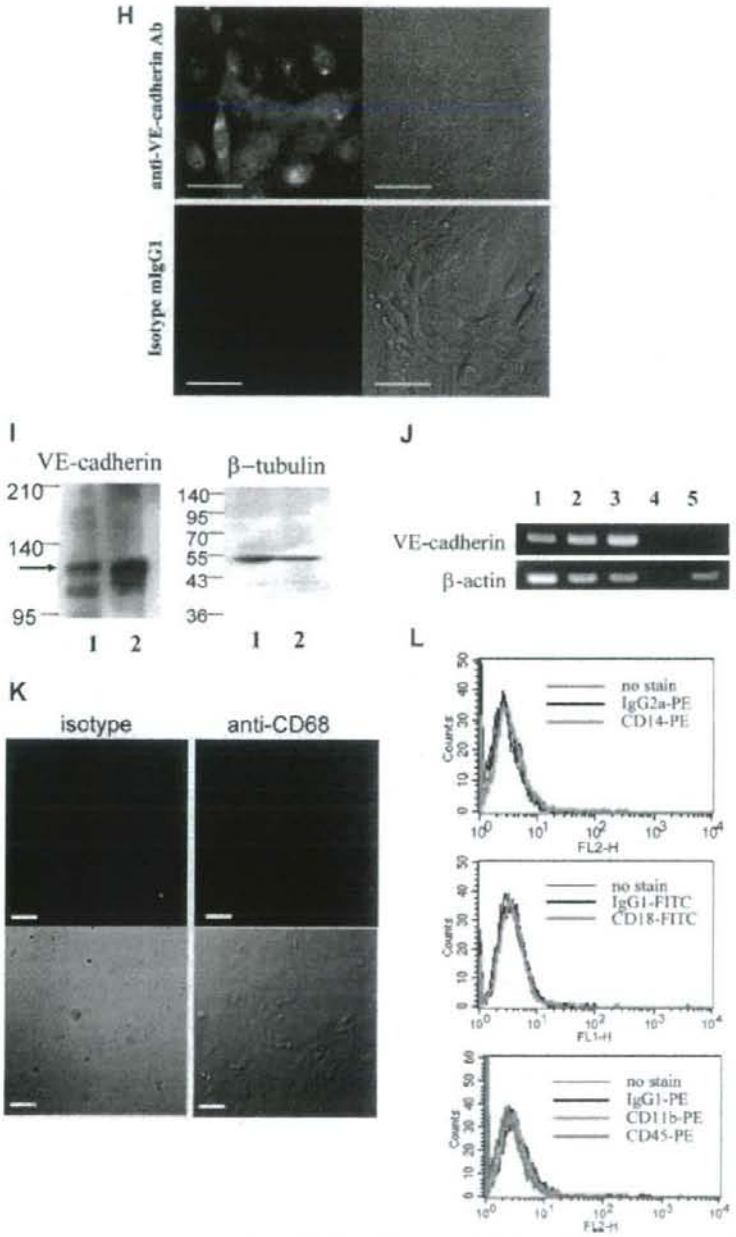

Fig. 6. ***(Continued)***

human ES-derived endothelial cells to clinical purposes in future.

Technically, our differentiation method has two unique points. One is the two-step protocol, where a sphere formation is followed by adherent culture. Although a short sphere-forming process was performed in our system, we could obtain clear microscopic fields owing to the subsequent adherent culture step, during which cells proliferated and

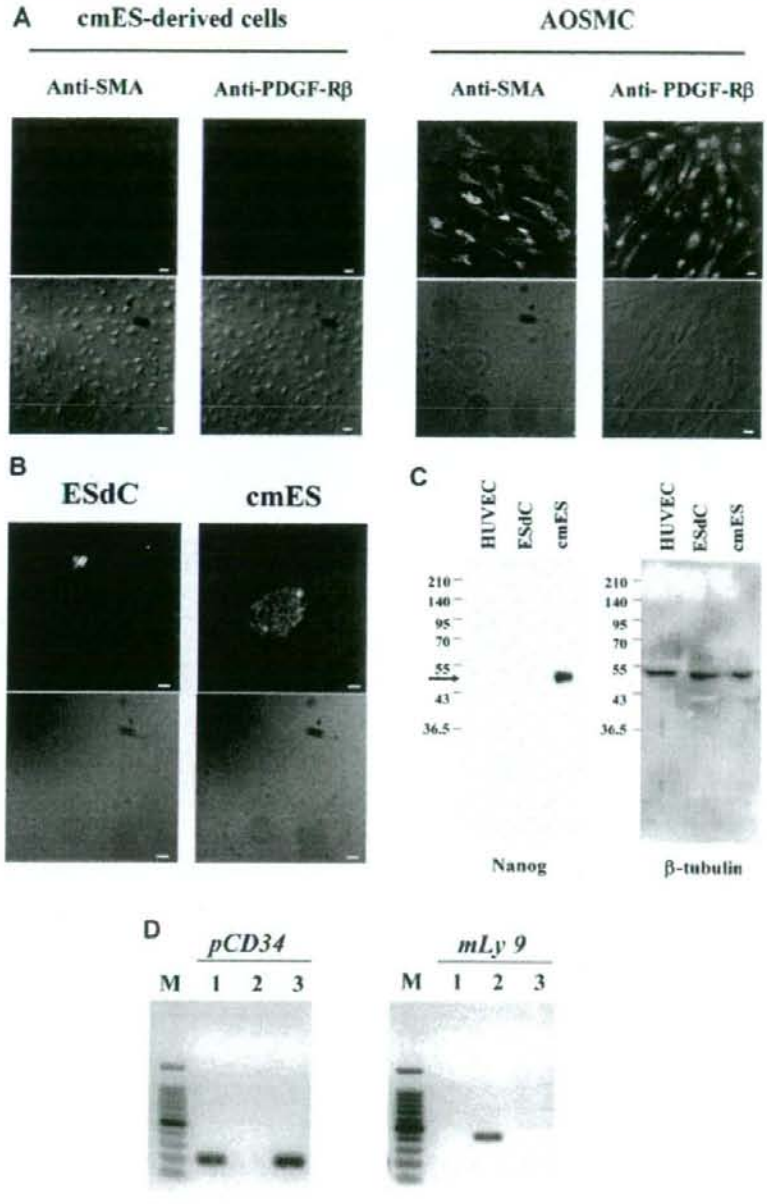

Fig. 7. Possible existence or contamination of pericytes, undifferentiated ES cells and MEFs was investigated. A: Possible existence of pericytes in cmES-derived cells was studied based upon smooth muscle specific markers (SMA and PDGF-Rβ). cmES-derived cells (left parts) were fixed and stained by anti-SMA antibody or anti-PDGF-Rβ antibody as indicated. As a positive control, human aortic smooth muscle cells (AOSMC) were used. The scale bar indicates 20 μm. B,C: Possible existence or contamination of undifferentiated cmES cells in cmES-derived cells (ESdC) was studied based upon undifferentiated ES cell marker, Nanog. The ESdC or undifferentiated cmES cells were fixed and stained by anti-human Nanog antibody (B) or were lysed and subjected to Western blotting using anti-Nanog antibody (C, left). An arrow indicates the expression of 50-kDa Nanog protein. For internal control, β-tubulin expression was examined (C, right). The scale bar indicates 100 μm. D: Possible contamination of MEFs in cmES-derived cells was studied using primate and murine specific markers. Genomic DNA was extracted from HUVECs (lane 1), MEFs (lane 2), and cmES-derived cells (lane 3). PCR was performed using the primers for primate CD34 genomic fragment (left column; *pCD34*) or those for murine ly 9.2 genomic fragment (right column; *mLy9*).

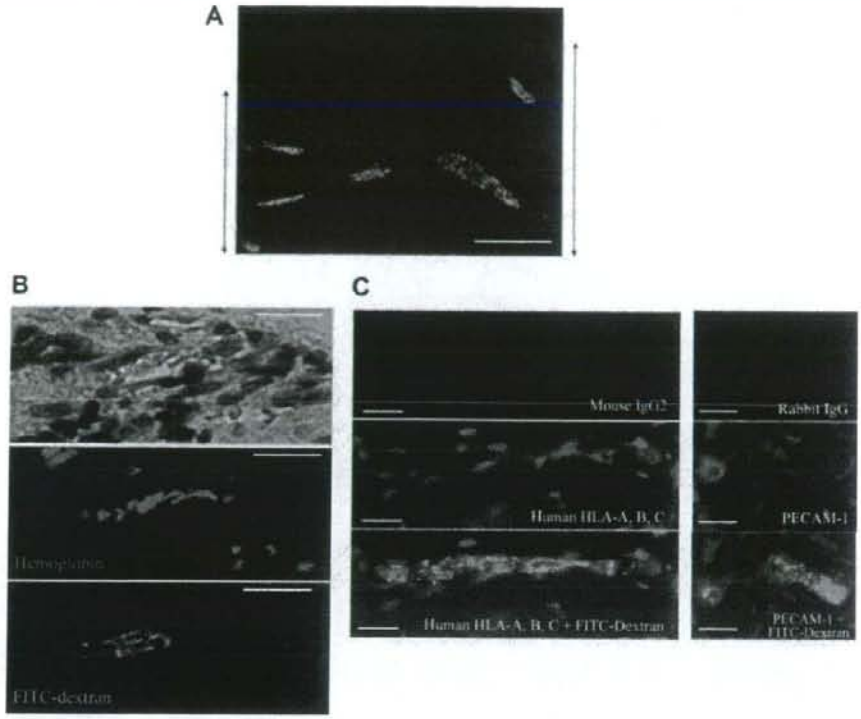

Fig. 8. The in vivo functions of cmES-derived cells. cmES-derived cells were cultured in honeycomb collagen sponges for 2 days in vitro and were then transplanted intraperitoneally into SCID mice. At day 35, FITC-dextran was injected into the transplanted mouse from a tail vein. Then collagen plugs were taken out, fixed, embedded and sliced as described in Materials and Methods Section. A: Fluorescence microscopic observations of FITC-dextran in sliced honeycomb collagen sponges. The scale bar indicates 100 μm. B: The microscopic observation of hematoxylin-eosin-stained samples (upper) and fluorescence microscopic observations of autofluorescence of hemoglobins (middle) and FITC-dextran (lower). Scale bars indicate 20 μm. C: Immunostaining studies were performed using indicated antibodies. The positive staining by anti-human PECAM-1 and anti-human HLA-A, B, C antibodies indicates the recruitment of cmES-derived cells into the neovascularity. Scale bars indicate 20 μm.

spread out almost like a monolayer culture. Hence, we could identify a unique construction, a sac-like structure surrounded by cobblestone cells, as the parental organization for vascular endothelial cells. Recently, the existence of this "sac-like" structure was independently reported (Ma et al., 2007), where human ES cells were co-cultured with murine OP9 stromal cells. Interestingly, they reported that the sac-like structures emerged with the same time course (around 12 days after co-culture) as our system. Because we applied the feeder-free culture method, we could detect the presence of surrounding cobblestone cells, which might possibly be merged with OP9 cells in their system. By immunostaining studies, we further noticed that both sac wall cells and surrounding cobblestone cells expressed VE-cadherin at intercellular junctions (Fig. 1D).

Another point of our success may reside in the formula of our differentiation medium. In contrast to previous reports, where a commercially available vascular endothelial cell-specific medium of EGM®-2 MV BulletKit was used (Kaufman et al., 2004; Wang et al., 2007), we prepared the differentiation medium by modifying the culture medium optimized to hematopoietic differentiation (Li et al., 2001). As our original aim was to produce hematopoietic stem cells, we deleted GM-CSF, G-CSF, erythropoietin and hydrocortisone, which rather work in later and mature phases of hematopoiesis, from the formula by Li et al. (2001). After we had established our method for high efficiency differentiation of vascular endothelial cells, we re-evaluated the necessity of each cytokine and found that the differentiation medium was indeed optimal. Among six cytokines, the role of VEGF is very clear: it is required for production of cell surface VE-cadherin/PECAM-1-positive population. Other cytokines including BMP-4, IL-3, IL-6, SCF and FLt3-L are required for the better performance of differentiation. Literally, BMP-4 is required for the generation of Scl/Tal-1-positive hemangioblast cells from murine ES cells (Park et al., 2004). IL-3 and SCF are reportedly effective in inducing vascular endothelial cells from murine hematopoietic cells (Yamada and Takakura, 2006). Recently, it was reported that IL-6 promotes choroidal neovascularization (Izumi-Nagai et al., 2007). Thus, it seems that every hematopoietic cytokine is involved in specific phase of vascular endothelial differentiation although its precise roles are not yet determined. Our usage of multiple hematopoietic cytokines possibly contributed to the prevention of emergence and/or proliferation of pericytes, which are often generated with vascular endothelial cells during